

1-1-1994

Finite element analysis of permanent indentation of solids due to low velocity impact

Sarath Abayaweera
University of Nevada, Las Vegas

Follow this and additional works at: <https://digitalscholarship.unlv.edu/rtds>

Repository Citation

Abayaweera, Sarath, "Finite element analysis of permanent indentation of solids due to low velocity impact" (1994). *UNLV Retrospective Theses & Dissertations*. 434.
<http://dx.doi.org/10.25669/rrts-5473>

This Thesis is protected by copyright and/or related rights. It has been brought to you by Digital Scholarship@UNLV with permission from the rights-holder(s). You are free to use this Thesis in any way that is permitted by the copyright and related rights legislation that applies to your use. For other uses you need to obtain permission from the rights-holder(s) directly, unless additional rights are indicated by a Creative Commons license in the record and/or on the work itself.

This Thesis has been accepted for inclusion in UNLV Retrospective Theses & Dissertations by an authorized administrator of Digital Scholarship@UNLV. For more information, please contact digitalscholarship@unlv.edu.

INFORMATION TO USERS

This manuscript has been reproduced from the microfilm master. UMI films the text directly from the original or copy submitted. Thus, some thesis and dissertation copies are in typewriter face, while others may be from any type of computer printer.

The quality of this reproduction is dependent upon the quality of the copy submitted. Broken or indistinct print, colored or poor quality illustrations and photographs, print bleedthrough, substandard margins, and improper alignment can adversely affect reproduction.

In the unlikely event that the author did not send UMI a complete manuscript and there are missing pages, these will be noted. Also, if unauthorized copyright material had to be removed, a note will indicate the deletion.

Oversize materials (e.g., maps, drawings, charts) are reproduced by sectioning the original, beginning at the upper left-hand corner and continuing from left to right in equal sections with small overlaps. Each original is also photographed in one exposure and is included in reduced form at the back of the book.

Photographs included in the original manuscript have been reproduced xerographically in this copy. Higher quality 6" x 9" black and white photographic prints are available for any photographs or illustrations appearing in this copy for an additional charge. Contact UMI directly to order.

UMI

A Bell & Howell Information Company
300 North Zeeb Road, Ann Arbor, MI 48106-1346 USA
313/761-4700 800/521-0600

**FINITE ELEMENT ANALYSIS OF PERMANENT
INDENTATION OF SOLIDS DUE TO
LOW VELOCITY IMPACT**

by

Sarath Abayaweera

A thesis submitted in partial fulfillment of
the requirements for the degree of

Master of Science

in

Mechanical Engineering

Department of Mechanical Engineering
University of Nevada, Las Vegas
May 1995

UMI Number: 1374863

UMI Microform 1374863
Copyright 1995, by UMI Company. All rights reserved.

**This microform edition is protected against unauthorized
copying under Title 17, United States Code.**

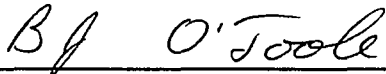
UMI

**300 North Zeeb Road
Ann Arbor, MI 48103**

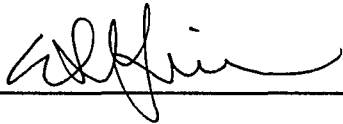
The Thesis of **Sarath Abayaweera** for the degree of Master of Science in
Mechanical Engineering is approved.



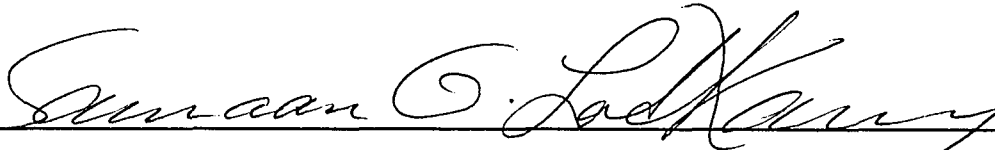
Chairperson, Mohamed B. Trabia, Ph.D.



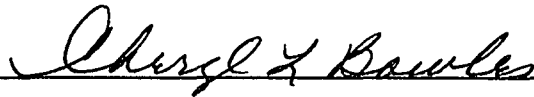
Examining Committee Member, Brendan J. O'Toole, Ph.D.



Examining Committee Member, Woosoon Yim, Ph.D.



Graduate Faculty Representative, Samaan G. Ladkany, Ph.D.



Graduate Dean, Cheryl L. Bowles, Ed.D.

University of Nevada, Las Vegas

April 1995

ABSTRACT

A finite element model for the seventy five ton multi-barrier multi-purpose canister (MPC) Overpack is developed. This model is subjected to an impact loading that produces plastic stresses. The finite element software COSMOS/M 1.7 is used to study the nonlinear behavior of the canister overpack. A new mechanism for energy absorption is adopted to determine the permanent indentation. The results of the analysis for nodal displacements and stresses, along with the energy of impact, are used to evaluate the permanent indentation. COSMOS/M analysis yielded acceptable values for the permanent indentation for the impact of plane cylinders within a reasonable range of velocities. For the MPC Overpack, the FEM method produced values that appear reasonable, but there is no valid comparison. FEM method can be used as a guidance within limitation to ascertain the reuse of the MPC Overpack.

TABLE OF CONTENTS

ABSTRACT.....	iii
LIST OF FIGURES	vii
ACKNOWLEDGEMENTS	ix
CHAPTER 1 INTRODUCTION	
1.1 Purpose of the Study	1
1.2 Literature Survey	1
CHAPTER 2 CONTINUOUS FORCE MODEL FOR ELASTIC-PLASTIC IMPACT OF SOLIDS	
2.1 Introduction	5
2.2 Analysis of Force and Displacement in the Compression Phase	6
2.3 Analysis of Force and Displacement in the Restitution Phase.....	8
2.4 Summary.....	12
CHAPTER 3 IMPACT ANALYSIS OF CYLINDERS	
3.1 Objective.....	14
3.1.1 Theoretical Minimum Force required to produce Plastic Deformation.....	14
3.1.2 Force Displacement Relation.....	16
3.1.3 Theoretical Minimum Velocity required to produce Plastic Deformation.....	17
3.1.4 Determination of Permanent Indentation.....	17
3.2 FEM Modeling of Plane Cylinders.....	19
3.2.1 Introduction.....	19
3.2.2 Element Group and Material Properties.....	20
3.2.3 Geometric Modeling of Cylinders.....	23
3.2.4 Meshing of Quadrilateral Elements	23
3.2.5 Boundary Conditions	24
3.2.6 Impact Force.....	25
3.2.7 Gap Lines and Gap Elements	26
3.3 FEM Impact Analysis of Plane Cylinders	27

3.3.1 FEM Minimum Force required to produce Plastic Deformation.....	27
3.3.2 Elastic Impact Analysis	28
3.3.3 FEM Minimum Velocity required to produce Plastic Deformation.....	29
3.3.4 Plastic Impact Analysis	29
3.3.5 FEM determination of the Permanent Indentation.....	31
3.4 Comparison of Results	32
CHAPTER 4 IMPACT ANALYSIS OF THE MPC OVERPACK	
4.1 Objective.....	36
4.1.1 Force Displacement Relation.....	36
4.1.2 Theoretical Minimum Force required to produce Plastic Deformation.....	40
4.1.3 Theoretical Minimum Velocity required to produce Plastic Deformation.....	40
4.1.4 Determination of Permanent Indentation.....	40
4.2 FEM Modeling of MPC Overpack	42
4.2.1 Multi Purpose Canister Overpack	42
4.2.2 FEM Modeling of MPC Overpack.....	43
4.2.3 Impacting Object	45
4.2.4 Boundary Conditions	45
4.2.5 Gap Surfaces and Gap Elements.....	47
4.2.6 Non linear Static Analysis.....	48
4.3 FEM determination of the Permanent Indentation.....	49
4.3.1 Elastic Analysis.....	49
4.3.2 FEM Minimum Force required to produce Permanent Indentation.....	50
4.3.3 FEM Minimum Velocity required to produce Plastic Deformation.....	50
4.3.4 Plastic Analysis.....	51
4.4 Comparison of Results.....	53
CHAPTER 5 CONCLUSIONS AND RECOMMENDATIONS	
5.1 Conclusions.....	58
5.2 Recommendations.....	59
APPENDIX I DESCRIPTION OF COSMOS/M 1.7 FEM SOFTWARE APPLICATIONS	60
APPENDIX II COSMOS/M CODE FOR PLANE CYLINDERS.....	65
APPENDIX III MATHCAD CALCULATIONS FOR PLANE CYLINDERS.....	69

APPENDIX IV COSMOS/M CODE FOR SPHERE AND CYLINDER.....	73
APPENDIX V FORTRAN PROGRAM TO CALCULATE STRESS*VOLUME....	85
APPENDIX VI TABLES OF DATA.....	107
APPENDIX VII MATHCAD CALCULATIONS FOR SPHERE AND CYLINDER.....	110
BIBLIOGRAPHY.....	113

LIST OF FIGURES

Figure 2.1 Contact Force vs Displacement	10
Figure 3.1 Deformed shape of Cylinders.....	17
Figure 3.2 Theoretical Variation of Coefficient of Restitution with Impact Velocity.....	19
Figure 3.3 Contact of two Cylinders due to an Impacting Force	21
Figure 3.4 Y_d/Y_s versus 0.2 % Compressive Proof Stress.....	22
Figure 3.5 Stress-Strain Curve.....	23
Figure 3.6 COSMOS/M Quadrilateral Meshing of the Cylinders.....	24
Figure 3.7 Boundary Conditions on Cylinders	25
Figure 3.8 Force on the movable Cylinder (right)	26
Figure 3.9 Location of Gaps and Gap Elements.....	27
Figure 3.10 Relation between the Applied Load and the Contact Node Displacement	29
Figure 3.11 Relation between the Gap Height and the Contact Node Displacement	30
Figure 3.12 Relation between the Average Stress of the Contact Nodes and Contact Node Displacement	31
Figure 3.13 FEM Variation of Coefficient of Restitution with Impact Velocity...	32
Figure 3.14 Comparison of Theoretical and FEM values for Maximum Compression, Force, Coefficient of Restitution, and Permanent Indentation.....	33
Figure 4.1 Contact of Solid Sphere and Solid Cylinder due to an Impacting Force.....	37
Figure 4.2 Theoretical variation of Coefficient of Restitution with Impact Velocity.....	42
Figure 4.3 MPC Overpack - Sectional View.....	44
Figure 4.4 Sphere in contact with MPC Overpack.....	44
Figure 4.5 FEM Model of Sphere and Cylinder in contact.....	46
Figure 4.6 Sphere in contact with Cylinder.....	46
Figure 4.7 Closeup view of the contact region.....	47
Figure 4.8 Three by three Gap Surface on Sphere.....	48
Figure 4.9 Relation between Applied load and the Contact Node Displacement.....	50
Figure 4.10 Relation between the Energy Absorbed during the Impact and Contact Node Displacement.....	51

Figure 4.11 Relation between the FEM Coefficient of Restitution and Impact Velocity.....	53
Figure 4.12 Comparison of Theoretical and FEM values for Maximum Compression, Force, Coefficient of Restitution, and Permanent Indentation.....	55

ACKNOWLEDGEMENTS

In this endeavor I wish to express my gratitude to Dr. Mohamed Trabia, for being my advisor and for his guidance. I sincerely thank him for all the help and the time he has given me to make this thesis a success. His knowledge, attitude towards research and the personal touch have always inspired me to do my best. I am also very grateful to Dr. Samaan Ladkany, my graduate faculty representative, for consenting to be on the committee and for providing me with financial support through UNLV/DOE project during the summer.

I am deeply indebted to Dr. Brendan O'Toole for being my committee member. I owe much gratitude to Dr. Woosoon Yim, for consenting to be on the examining committee inspite of his busy schedule.

I wish to thank all of my friends in UNLV/DOE project for being helpful during this rather brief encounter. I acknowledge with gratitude, the help and moral support my mother and my brothers offered me during the course of this work.

CHAPTER 1

INTRODUCTION

1.1 Purpose of the Study

The objective of this study is to formulate a theory for the energy absorption during impact and use finite element method to determine the resulting amount of permanent indentation. This information is used as a basis in future studies to assess the extent of the damage to the impacting bodies.

In transporting or moving a solid object such as a nuclear waste canister, there is a possibility of collision or impact with other solid objects. Collisions usually result in damage to the impacting bodies. The degree of damage is important in cases where the integrity of the colliding bodies can cause severe damage to humans, or to the environment. It is therefore, necessary to analyze the impact, and assess the damage especially in the case of a nuclear waste canister overpack (outer casing of canister) to determine whether it is safe to reuse.

1.2 Literature Survey

The first satisfactory analysis of contact stresses of elastic solids was presented by Hertz (1882). In addition to static loading he also investigated the quasi-static impacts of spheres. Hertz attempted to use his theory to give a precise

definition of hardness of a solid in terms of the contact pressure to initiate plastic yield in the solid. This definition was proved to be unsatisfactory because of the difficulty of detecting the point of first yield under the action of contact stress.

A satisfactory theory of hardness had to wait for development of the theory of plasticity.

During the last four decades, elastic plastic mechanics has received a lot of attention. A number of investigators as early as 1952 concentrated their efforts on plastic behavior of materials. Crook (1952) derived a model using plasticity as a means for energy dissipation. He compared his results with experimental studies. Classical approach to the problem of impact between two solids, Meirovitch (1970) and Brach (1991), assumes that impact occurs instantaneously. It uses parameters of motion before impact, momentum equations and coefficient of restitution to determine the parameters of motion after impact. This method depends on the coefficient of restitution. Khulief and Shabana (1986) and Lankarani and Nikravesh (1992), extended this approach to multi-body systems. However, experimental evidence indicates that the coefficient of restitution is dependent on the material, impact velocity, etc., Goldsmith (1960). Adams et al. (1993) presented a simple procedure for predicting the motion of two colliding rigid bodies immediately after impact. This procedure gives the effective approach velocity in terms of the actual approach velocity, the coefficient of friction and the location of the impact point with respect to the mass centers. Alternative to instantaneous impact assumption, various continuous force models have been

proposed. In this analysis it is assumed that a continuous force acts throughout the duration of impact and is included in the equations of motion. The value of the coefficient of restitution and duration of impact is determined using energy balance. Khuleif and Shabana (1987) suggested a spring-damper model. Some investigators proposed models based on the Hertz contact stress. In a Hertz contact force problem, contact surface is planar and bodies exhibit small strains outside the contact surface. Different energy dissipation mechanisms were suggested. Barnhart and Goldsmith (1957) developed theory for transverse impact of spheres on elastic impact using force indentation law and linear elastic boundary conditions. Lankarani and Nikravesh (1989) developed a hysteresis damping coefficient that is appropriate for impact at low speeds. Several models were proposed for elastic-plastic contact problem. Goldsmith (1960) as well as Jhonson (1985) derived equation for coefficient of restitution by introducing different compliance relations. A finite element method for Hertz contact-impact problems was proposed by Chan et al. (1971) and Hughes et al. (1976). Chan et al. provided a finite element method solution to two identical cylinders in contact. They inferred that the results agreed quite well with the Hertz solution at higher loads. The explanation given for the discrepancy at lower loads is that there are fewer elements and nodal points on the contact surfaces. Lankarani and Nikravesh (1992) presented a method for determining permanent indentation, duration of impact, and force history when the coefficient of restitution is known. They assumed that compression time is equal to restitution time and did not consider the

material dynamic yield strength. A finite element approach for shape optimization in two-dimensional frictionless contact problems was presented by Fancello et al. (1994). They concentrated on the optimum shape that gives a constant distribution of stresses along the contact boundary. This approach takes into consideration that the finite element method gives low accuracy on the boundaries. Weissman et al. (1993) used two-dimensional elastoplastic problems to assess the performance of a family of mixed finite elements in the non-linear regime. They used four node bilinear quadrilateral elements that exhibit high accuracy in coarse meshes to simulate plane stress, plane strain, axisymmetric and (shear-deformable) plate bending problems. A continuous force model for elastic-plastic impact of solids was presented by Trabia (1993). This analysis does not assume the coefficient of restitution and instead considers relative velocity of the impacting bodies in the equations of motion. In this thesis, these concepts were extended to use finite element method to evaluate the permanent indentation. The finite element software COSMOS/M version 1.7 is used to model the geometry of the impacting bodies and analyze the resulting deformation.

CHAPTER 2

CONTINUOUS FORCE MODEL FOR ELASTIC-PLASTIC IMPACT OF SOLIDS

2.1 Introduction

Impact between two solids are either elastic or plastic. In elastic impact no permanent deformation occurs. In plastic impact, some energy is absorbed by the solids resulting in permanent indentation.

Impact can be divided into two phases. The first phase is the compression phase. In this phase the relative velocity between the two bodies is equal to zero. If friction between the two bodies is negligible, then all kinetic energy is transformed into elastic energy. This energy is manifested as compression in the direction normal to impact direction. The second phase is the restitution phase. This phase starts after the compression reaches its maximum value. This phase may be elastic or plastic.

In this chapter, the equations derived by Trabia (1993) are discussed. Trabia presented a Hertz-type force model and proposed a model for energy absorption in the impacted solids. This model is valid for the cases when plasticity accounts for the absorption of energy during impact. It is assumed that impact forces follow continuous Hertz contact force model. This method yields the

coefficient of restitution, permanent indentation, and impact time. It also determines the value of the relative velocity after which the plastic indentation occurs.

2.2 Analysis of Force and Displacement in the Compression Phase

In this phase it is assumed that the force between the two bodies acts as a nonlinear spring, whose equation is given by,

$$F = K z^n \quad (2.1)$$

Where, F - impact force between the two solids

K - Stiffness of the nonlinear spring

z - elastic displacement

n - nonlinear spring power

K is a function of the modulus of elasticity and diameter, and n depends on the geometry of the two bodies.

Using, Newton's second law of motion, for the two bodies under normal impact, and substituting, $\alpha = z_1 + z_2$,

$$\ddot{\alpha} = \ddot{z}_1 + \ddot{z}_2$$

$$F = - m_1 \ddot{z}_1 = - m_2 \ddot{z}_2 = - \frac{m_1 m_2}{m_1 + m_2} \ddot{\alpha} \quad (2.2)$$

Where, m_i - mass of body i

z_i - displacement of body i along the impact direction

Combining equations 2.1 and 2.2,

$$-\frac{m_1 m_2}{m_1 + m_2} \ddot{\alpha} = K \alpha^n \quad (2.3)$$

The above equation is a second order differential equation and has the following initial conditions ($t = 0$).

$$\dot{\alpha} = v_0 \quad \alpha = 0 \quad (2.4)$$

Where, v_0 is the initial relative velocity.

Integrating with respect to α yields,

$$\frac{1}{2} \frac{m_1 m_2}{m_1 + m_2} (\dot{\alpha}^2 - v_0^2) = -\frac{K \alpha^{n+1}}{n+1} \quad (2.5)$$

Maximum compression occurs when,

$$\dot{\alpha} = 0 \quad (2.6)$$

Substituting the above in equation 2.5, the maximum compression (α_m), as shown in figure 2.1, is given by,

$$\alpha_m = \left(\frac{n+1}{2K} \frac{m_1 m_2}{m_1 + m_2} v_0^2 \right)^{\frac{1}{n+1}} \quad (2.7)$$

From equation 2.5, the following expression for the instantaneous velocity is obtained.

$$\alpha = \sqrt{-\frac{2 K \alpha^{n+1}}{n+1} \frac{m_1+m_2}{m_1 m_2} + v_0^2} \quad (2.8)$$

Integrating with respect to time and rearranging the above equation, the time of duration of the compression phase is given by,

$$\tau_1 = \int_0^{\alpha_m} \frac{1}{\sqrt{-\frac{2 K \alpha^{n+1}}{n+1} \frac{m_1+m_2}{m_1 m_2} + v_0^2}} d\alpha \quad (2.9)$$

Changing the variable to u such that,

$$u = \frac{\alpha}{\alpha_m}, \quad \text{gives} \quad \tau_1 = \frac{\alpha_m}{v_0} \int_0^1 \frac{1}{\sqrt{1-u^{n+1}}} du \quad (2.10)$$

At the limit $u = 1$, the velocity is zero and is about to change the direction of motion. This represents an unsteady state of rest. Since, u is defined as a ratio of displacements, it is a dimensionless parameter.

2.3 Analysis of Force and Displacement in the Restitution Phase

When impact between two bodies occur, the plastic indentation is related to the yield point of the softer body. Trabia in his paper used Tresca's maximum shear stress failure criterion for simplicity, and obtained the dynamic yield strength compiled in Goldsmith (1960).

The force F_p corresponding to the stress tensor that satisfies any failure

theory is evaluated. Observing the fact that, when the material just goes into plastic stage the relative velocity is zero, also, $\alpha = \alpha_m$, and $v_0 = v_p$, and simplifying equation 2.5,

$$-\frac{m_1 m_2}{m_1 + m_2} (-v_p^2) = -\frac{K \alpha_m^{n+1}}{n+1} \quad (2.11)$$

Substituting, $F_p = K \alpha_m^n$ in the above equation and simplifying,

$$v_p = \sqrt{F_p^{\frac{n+1}{n}} K^{-\frac{1}{n}} \frac{2}{n+1} \frac{m_1 + m_2}{m_1 m_2}} \quad (2.12)$$

After maximum compression occurs, the relation between force and displacement is given by,

$$F = F_m \left(\frac{\alpha - \alpha_p}{\alpha_m - \alpha_p} \right)^n \quad (2.13)$$

Where α_p (figure 2.1) is the value of permanent indentation. The above relation was experimentally obtained by Crook (1952).

The work done during the compression phase is given by,

$$W_c = \int_0^{\alpha_m} K \alpha^n d\alpha \quad (2.14)$$

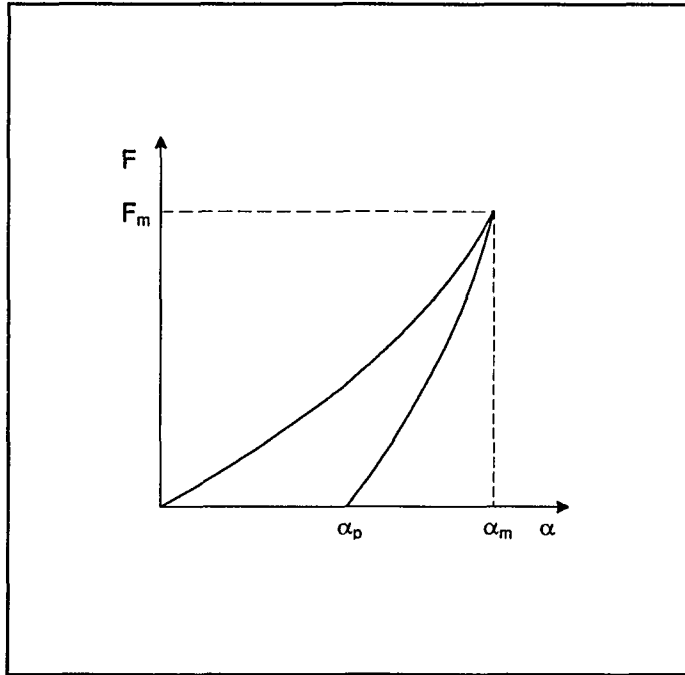


Figure 2.1 Contact Force vs Displacement

The work done during the restitution phase is given by,

$$W_r = \int_{\alpha_m}^{\alpha_p} F_m \left(\frac{\alpha - \alpha_p}{\alpha_m - \alpha_p} \right)^n d\alpha \quad (2.15)$$

Equating the work done by the impact force during both phases, to the energy absorbed by both bodies, the following expression is obtained.

$$\int_0^{\alpha_m} K\alpha^n d\alpha + \int_{\alpha_m}^{\alpha_p} F_m \left(\frac{\alpha - \alpha_p}{\alpha_m - \alpha_p} \right)^n d\alpha = \sum_{l=1}^2 \int_0^{\alpha_p} \left(\int_{A_l(z)} -\sigma_{z_l} dA_l(z) \right) dz \quad (2.16)$$

Where, σ_{zi} is the stress in the impact direction in body i at the indentation surface and $dA_i(z)$ is the area of indentation surface of body i . Integration with respect to z gives the energy absorbed.

Simplifying equation 2.16,

$$\frac{F_m \alpha_p}{n+1} = \sum_{i=1}^2 \int_0^{\alpha_p} \left(\int_{A_i(z)} -\sigma_{zi} dA_i(z) \right) dz \quad (2.17)$$

Equation 2.17 has one unknown α_p , which can be solved algebraically or numerically depending on the shape of the bodies.

Coefficient of restitution e , is defined as,

$$e = -\frac{v_1}{v_0} \quad (2.18)$$

Where, v_1 is the relative velocity after impact.

Equating the change in kinetic energy due to impact to the left-hand side of equation 2.17,

$$\frac{1}{2} \frac{m_1 m_2}{m_1 + m_2} v_0^2 (1 - e^2) = \frac{F_m \alpha_p}{n+1} \quad (2.19)$$

If the impact is fully elastic, then e equals one, and there is no loss in kinetic energy .

By comparing equation 2.7 and 2.19, the following expression is obtained.

$$\frac{\alpha_p}{\alpha_m} = 1 - e^2 \quad (2.20)$$

Writing the energy balance for the restitution phase,

$$-\int_{\alpha_m}^{\alpha_p} F_m \left(\frac{\alpha - \alpha_p}{\alpha_m - \alpha_p} \right)^n = \frac{1}{2} \frac{m_1 m_2}{m_1 + m_2} (\alpha^2 - 0) \quad (2.21)$$

Rearranging the above equation and integrating with respect to time, the following expression for restitution time (τ_2) is obtained.

$$\tau_2 = -\int_{\alpha_m}^{\alpha_p} \left[\frac{v_0^2}{\alpha_m} \left((\alpha_m - \alpha_p) - \frac{(\alpha - \alpha_p)^{n+1}}{(\alpha_m - \alpha_p)^n} \right) \right]^{-\frac{1}{2}} d\alpha \quad (2.22)$$

Changing the variable to u using the following substitution, and introducing e in the above equation,

$$u = \left(\frac{\alpha - \alpha_p}{\alpha_m - \alpha_p} \right), \text{ gives } \tau_2 = \frac{\alpha_m - \alpha_p}{v_0 e} \int_0^1 \frac{1}{\sqrt{1 - u^{n+1}}} du \quad (2.23)$$

As in the compression phase, u is a dimensionless parameter. At $u = 1$, the bodies are about to separate.

2.4 Summary

A model for elastic-plastic impact of solids is analyzed. This model is valid for the cases when plasticity accounts for the absorption of energy during impact. It is assumed that impact forces follow continuous Hertz contact force model. The model depends on a mechanism for energy absorption that yields the relative velocity of impact needed to initiate permanent deformation, coefficient of

restitution, and impact time.

CHAPTER 3

IMPACT ANALYSIS OF CYLINDERS

3.1 Objective

The objective of the theoretical analysis is to subject the two solid cylinders (axes parallel) in contact to a static loading and derive an expression to evaluate the permanent indentation. The results of the FEM analysis discussed in section 3.3, will be compared with the theoretical values. This analysis is performed as a preliminary study to ascertain whether it is feasible to conduct a similar FEM analysis on the MPC Overpack.

3.1.1 Theoretical Minimum Force required to produce Plastic Deformation

When curved elastic bodies are pressed together, finite contact areas are developed because of deflections. These contact areas are very small, however, the compressive stresses that are produced tend to be extremely high. The applied force produces a maximum contact pressure which exists on the load axis. The pressure distribution over the contact area varies with the geometry of the contacting bodies. The equations relating to the contact mechanics of two solid cylinders are discussed in the following paragraphs.

For two solid cylinders with their axes parallel, the minimum contact pressure

p_0 required to produce plastic deformation, Juvinal (1991) is given by,

$$p_0 = 0.564 \sqrt{\frac{F_p \left(\frac{1}{R_1} + \frac{1}{R_2} \right)}{L \Delta}} \quad (3.1)$$

Where,

$$\Delta = \frac{1-v_1^2}{E_1} + \frac{1-v_2^2}{E_2} \quad (3.2)$$

F_p - Minimum Force required to produce plastic deformation

R_1 - Radius of Cylinder 1

R_2 - Radius of Cylinder 2

L - Length of the Cylinders

v_1 - Poisson's Ratio of Cylinder 1

v_2 - Poisson's Ratio of Cylinder 2

E_1 - Modulus of Elasticity of Cylinder 1

E_2 - Modulus of Elasticity of Cylinder 2

For 1020 HR Steel, these values are,

$$E_1 = E_2 = 30 \times 10^6 \text{ lbf/in}^2 \quad v_1 = v_2 = 0.3 \quad \sigma_y = 42000 \text{ lbf/in}^2$$

$$\sigma_d = 2.6 \times \sigma_y$$

$$\sigma_d = 1.092 \times 10^5 \text{ lbf/in}^2$$

$$R_1 = R_2 = 1 \text{ inch}$$

Substituting, $p_0 = \sigma_d$, in equation 3.1 and solving for F_p ,

$$F_p = 1138 \text{ lbf}$$

3.1.2 Force Displacement Relation

When two cylindrical bodies with their axes parallel are pressed in contact by a force F per unit length, the problem becomes a two dimensional one. They make contact over a long strip of width $2a$. Using the Force-Displacement relation given by Juvinal (1991),

$$F = \frac{L}{1.13^2 \Delta} \left(\frac{1}{R_1} + \frac{1}{R_2} \right) a^2 \quad (3.3)$$

Where, (a) is as shown below.

The relation between the height (a) and displacement (z) , (figure 3.1) is given by,

$$a = \sqrt{2Rz - z^2} \quad (3.4)$$

Since, z is very small, z^2 can be neglected. Therefore, the equation reduces to,

$$a = \sqrt{2Rz} \quad (3.5)$$

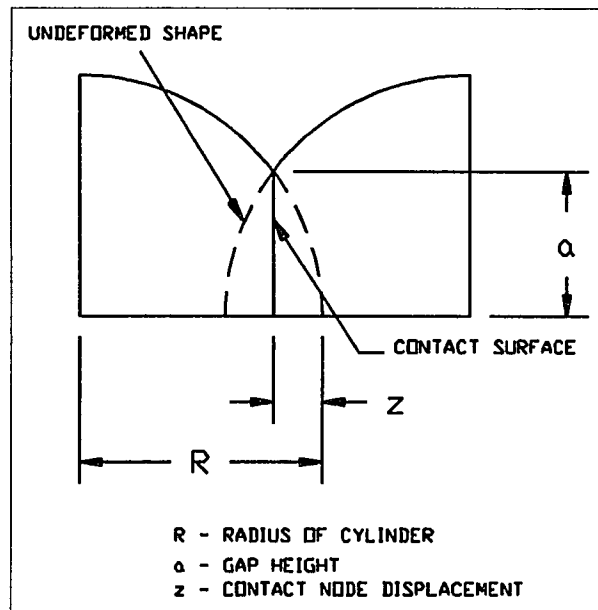


Figure 3.1 Deformed shape of Cylinders

Substituting for a^2 , in equation 3.3,

$$F = 3.2272 \times 10^6 z \quad (3.6)$$

Equation 3.6 is of the form, $F = K z^n$.

Therefore, $n = 1$, and $K = 3.2272 \times 10^6$ lbf/in

3.1.3 Theoretical Minimum Velocity to produce Plastic Deformation

The minimum velocity (v_p), required to produce plastic deformation is given by equation 2.12. Using, MathCad to solve,

$$v_p = 0.05 \text{ mph}$$

3.1.4 Determination of Permanent Indentation

Using, Juvinal's (1991) figure for the contact pressure distribution, the following equation is derived for σ_z , in the x, y plane (a - measured along y axis).

$$\sigma_z = \frac{p_0}{a} \sqrt{(a^2 - y^2)} \quad (3.7)$$

Johnson (1985) derived the expression for the maximum shear stress in terms of p_0 , and it is given by,

$$\tau_{\max} = \frac{p_0}{3.333} \quad (3.8)$$

Also, from Tresca's failure criterion, the following equation is derived,

$$\tau_{\max} = \frac{Yd}{2} \quad (3.9)$$

The energy absorbed by the cylinders is given by,

$$E = \sum_{l=1}^2 \int_0^z \int_{-a}^a \frac{p_0}{a} \sqrt{a^2 - y^2} dy dz \quad (3.10)$$

Substituting the above in equation 2.17, and solving, α_p is obtained.

The coefficient of restitution is evaluated using, equation 2.18.

The values for the impact velocity, permanent indentation and the coefficient of restitution are tabulated (Table 3.1). The following graph shows the variation of coefficient of restitution with impact velocity.

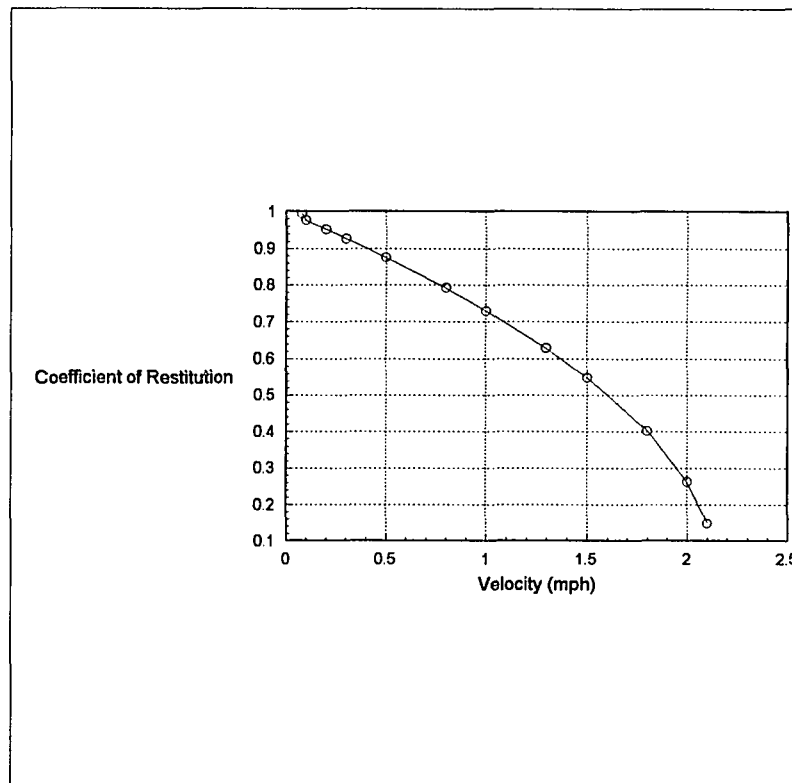


Figure 3.2 Theoretical Variation of Coefficient of Restitution with Impact Velocity

It can be seen from the above graph that, as the impact velocity increases, the coefficient of restitution decreases, which is expected.

3.2 FEM Modeling of Plane Cylinders

3.2.1 Introduction

Impact of two identical cylinders (figure 3.3) under plane stress conditions is analyzed using the Finite Element computer software COSMOS/M version 1.7. In this analysis, the information is written in COSMOS/M code using an editor and is saved as a source file. This source file containing the material properties, geometry, solution techniques etc., is called after activating the program. The

versatility and application features of COSMOS/M is given in greater detail in Appendix A.

The results of the impact analysis is used to evaluate the permanent indentation. The method of determining the permanent indentation is based on a new mechanism for energy absorption in the impacted bodies. This method yields the relative velocity of impact needed to initiate permanent deformation. The details of the analysis are discussed in the following paragraphs, and the results are compared with the theoretical solution.

3.2.2 Element Group and Material Properties

In the two dimensional analysis under plane stress conditions, COSMOS/M requires the element type be defined. For this purpose, EGROUP command is used to define the type (PLANE2D), solution technique (Full Integration), and the model type (Von Mises elasto-plastic, isotropic hardening). The REALCONST command is used to declare the thickness of the cylinder. The Modulus of Elasticity, Poisson's Ratio, Yield Stress etc., are defined under MPROP command.

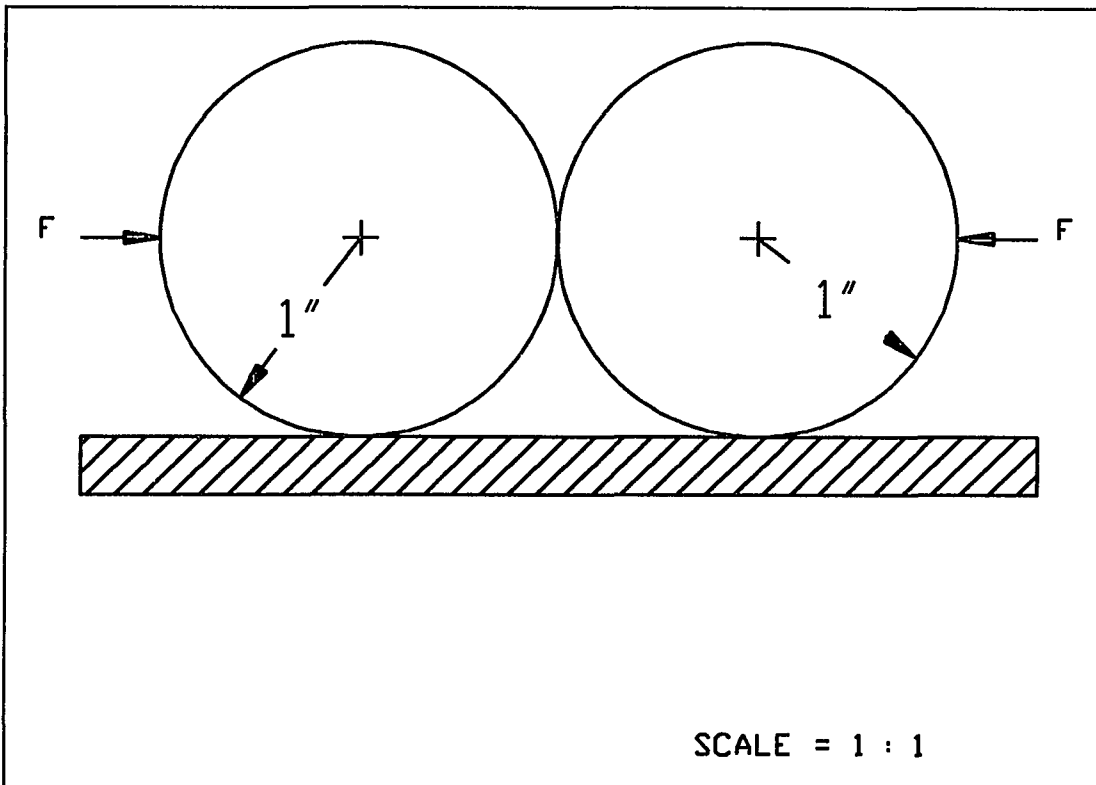


Figure 3.3 Contact of two Cylinders due to an impacting Force

Since, the purpose of this study is directly related to impact, it is important to consider the dynamic behavior of the material. Experimental evidence (Goldsmith 1960), shows that the dynamic yield stress for a given material is increased both with impact velocity and decrease in test temperature. Tests conducted by Goldsmith on mild steel indicates that the dynamic compressive yield stress is raised by a factor varying between two and three over the corresponding static yield stress. Goldsmith's experimental curves for the ratio Dynamic Yield Strength (Y_d)/Static Yield Strength (Y_s) versus 0.2 % Compressive Proof Stress (figure 3.4) a factor 2.6 for mild steel used in the impact model. The new value for the yield strength (Dynamic Yield Strength) is calculated by multiplying the Static

Yield Strength by a factor 2.6.

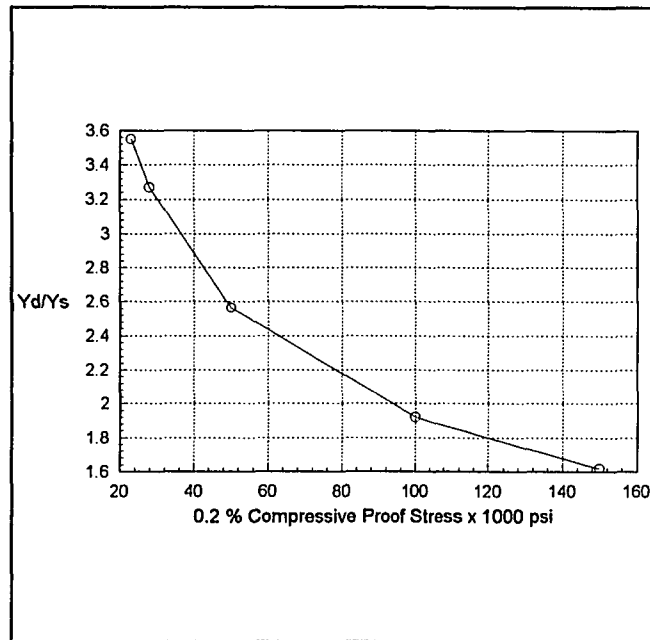


Figure 3.4 Yd/Ys versus 0.2 % Compressive Proof Stress

Another important declaration is the tangent modulus (figure 3.5). It is desired to keep the tangent modulus close to zero. This is achieved by the ETAN command. Since, COSMOS/M did not accept zero, a value of 1×10^6 lbf/in² is used.

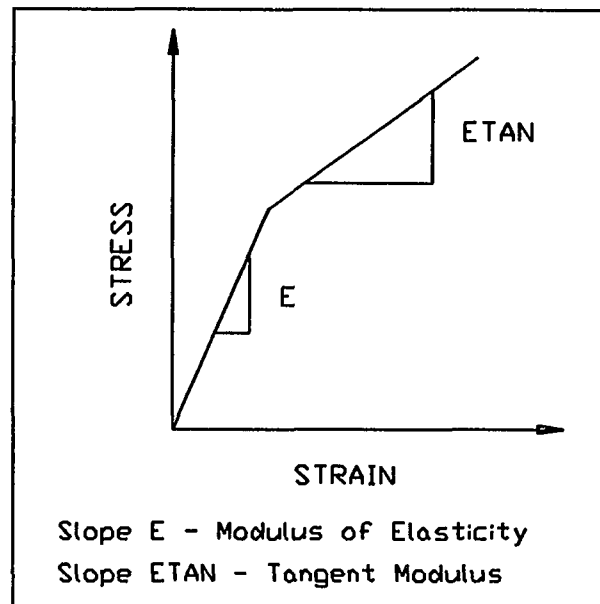


Figure 3.5 Stress-Strain Curve

3.2.3 Geometric Modeling of Cylinders

The computer software COSMOS/M 1.7 is a versatile package for structural analysis, which allows the user to create the geometry of the object under consideration, impose boundary conditions, and analyze stresses and strains when subjected to a loading. The package consists of different modules, which can be invoked within the program. The GEOSTAR module is the geometric modeler. This module is used in creating the geometry of the cylinders. Proper definition of geometry requires creation of points, curves, and surfaces. Because of geometric and loading symmetry of the impacting bodies, a quarter of a cylinder is modeled and is sufficient for nonlinear static analysis.

3.2.4 Meshing of Quadrilateral Elements

The accuracy of FEM analysis depends mainly on mesh density of the

model around the area under observation. In order to achieve a finer mesh around the point of contact, the plane of the cylinder is divided into three surfaces (figure 3.6). A finer quadrilateral mesh is obtained using M_SF command on the surface which contains the point of contact. The element size is approximately one fortieth of an inch.

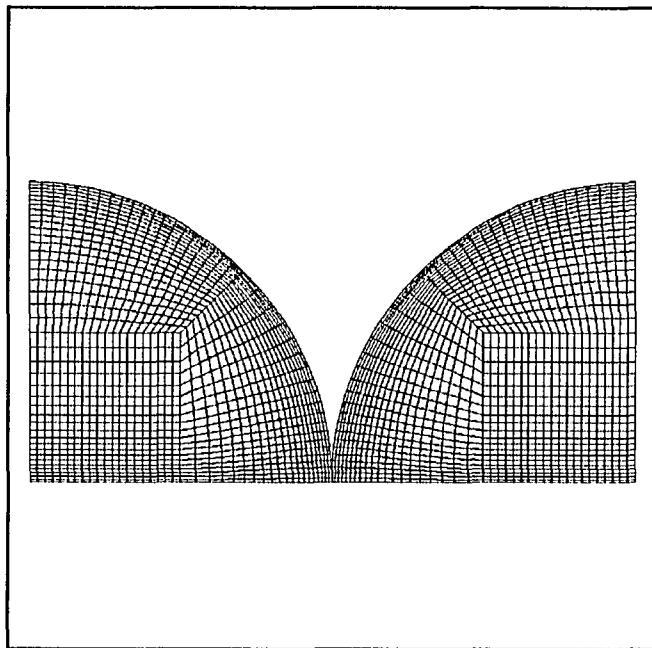


Figure 3.6 COSMOS/M Quadrilateral Meshing of Cylinders

3.2.5 Boundary Conditions

COSMOS/M program requires structural stability of the model for analysis. This is achieved by imposing the necessary and sufficient boundary conditions on the two cylinders. In this problem, the two cylinders are resting on

the ground, so that there is no motion in the vertical direction of the part which is in contact with the ground. It is also required that one cylinder is restricted to move in the horizontal direction to prevent sliding (figure 3.7). The displacement boundary conditions are imposed using the DCR command.

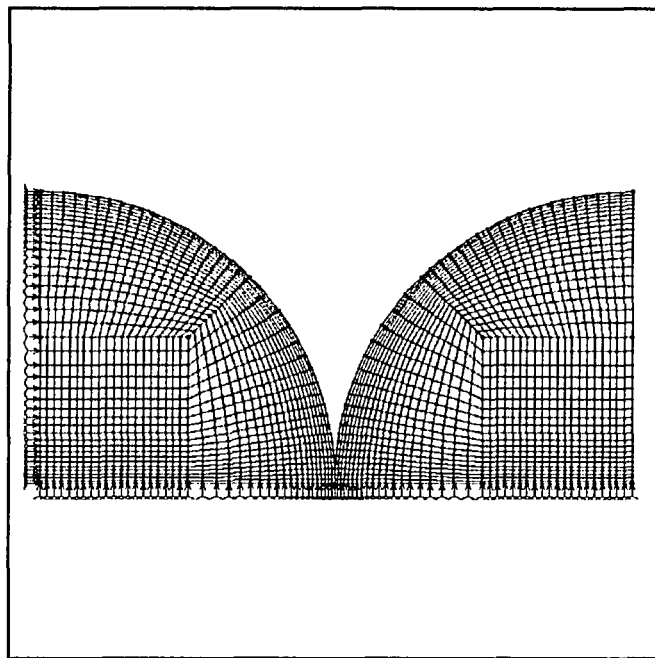


Figure 3.7 Boundary Conditions on Cylinders

3.2.6 Impact Force

The total impact force is distributed equally on the nodes of the line where the force acts (figure 3.8). This is achieved using the FCR (force on curve) command.

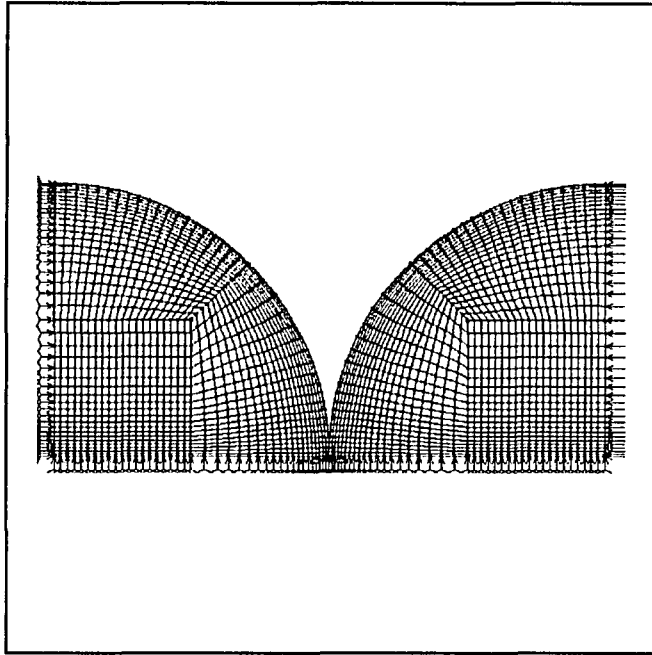


Figure 3.8 Force on movable Cylinder (right)

3.2.7 Gap Lines and Gap Elements

A gap is defined by two nodes. An open gap has no effect on the response of the structure while a closed gap, if rigid, limits the relative displacements of its two nodes. In 2D problems, a gap line is defined, and in a 3D problem a gap surface is defined (figure 3.9). Several methods have been developed to solve contact problems. COSMOS/M uses a hybrid technique which is different from the penalty method. This method does not require assigning penalty values and keeps the matrices size and bandwidth unchanged. In this method the displacement and the force method are combined to solve the matrix equation. The displacement method requires the nodal forces to be prescribed while, the force method requires the nodal

displacements to be prescribed. In general purpose finite element programs, a displacement - based method is used. However, in dealing with nonlinearities, such contact, a hybrid method can be efficient. A contact problem is considered as a general case of a gap problem. Two node gap elements are used in 2D and 3D contact problems, where bodies are coming in contact with each other due to the application of external forces.

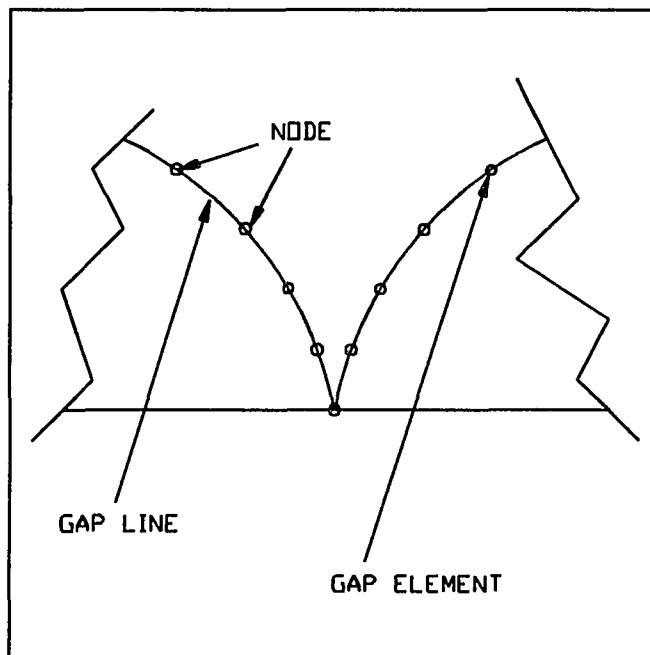


Figure 3.9 Location of Gap lines and Gap Elements

3.3 FEM Impact Analysis of Plane Cylinders

3.3.1 FEM Minimum Force required to produce Permanent Deformation

The minimum force F_p is determined by subjecting the model to different

loads and observing the maximum stress developed in bodies. When the maximum stress developed is very close to the dynamic yield, the load that produced it, is the value of F_p . The observed value is, 902 lbf, compared to the theoretical value 1138 lbf.

3.3.2 Elastic Impact Analysis

Non-linear analysis is performed on the model for the elastic load F_p using the command R_NONLINEAR, over a solution time of equal increments (linear force curve), and the material properties are as discussed in section 3.2. The results of the analysis for displacement of contact node along the direction of the force and the corresponding force value is then plotted and curve fitted using regression analysis.

The purpose of the elastic analysis is to determine the non-linear spring stiffness K and the non-linear spring power n from the regression data. The value K remains constant for the same material and n for the same geometry. For COSMOS/M elastic analysis (Appendix II), a force of 820 lbf ($<F_p$) is used to ensure that no plastic stresses are produced. The results of the analysis for the displacement of the contact node and the applied load are tabulated (Table 3.3.2-Appendix VI). The following graph shows the Force-Displacement relation.

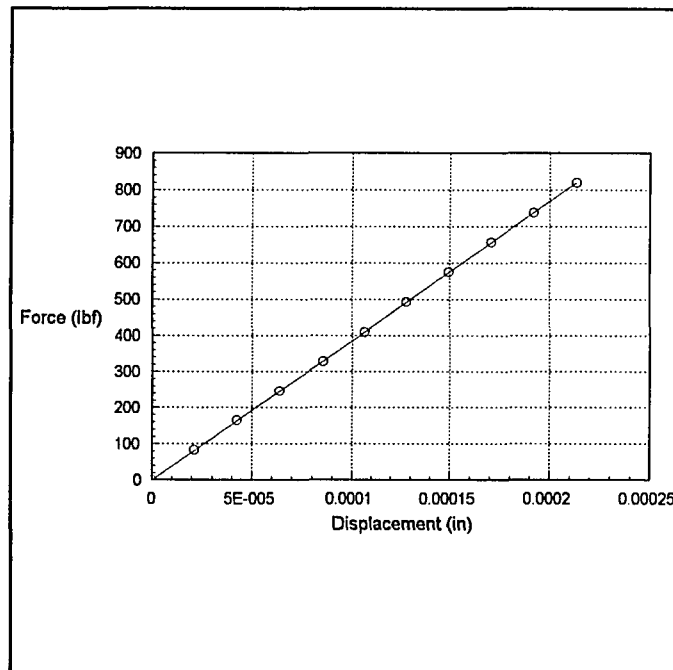


Figure 3.10 Relation between Applied Load (F) and Contact Node Displacement (z)

From regression analysis,

$$n = 1, \quad K = 3.8441 \times 10^6 \text{ lbf/in}$$

3.3.3 FEM Minimum Velocity to produce Plastic Deformation

Substituting for F_p , K , and n in equation 2.12,

$$v_p = 0.08 \text{ mph}$$

3.3.4 Plastic Impact Analysis

The model is subjected to a larger impacting force which produces plastic stresses, and non-linear analysis performed in the same manner as for elastic analysis. The results for number of gaps closed (explained in section 3.2) and the corresponding displacement of the contact node along the direction of the force is observed. Average contact stress over the closed gaps is evaluated for

each time step. The purpose of this analysis is to determine a relation between the gap height and the contact node displacement, and the average contact stress. These relations are then used in equation 2.17 to determine the permanent indentation.

For COSMOS/M analysis a load of 24600 lbf is used to produce plastic stresses. The results of the analysis is tabulated (Table 3.3.4-Appendix VI).

A plot of the data is given below.

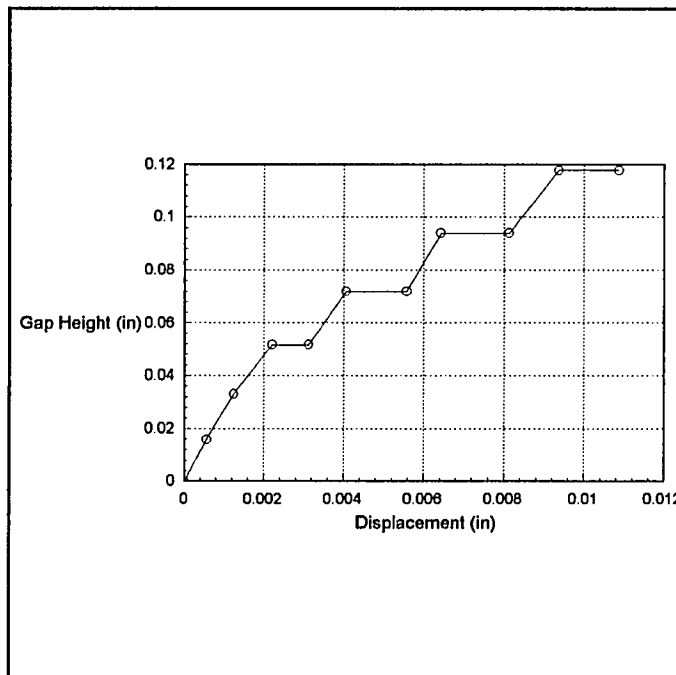


Figure 3.11 Relation between Gap Height (a) and Contact Node Displacement (z)

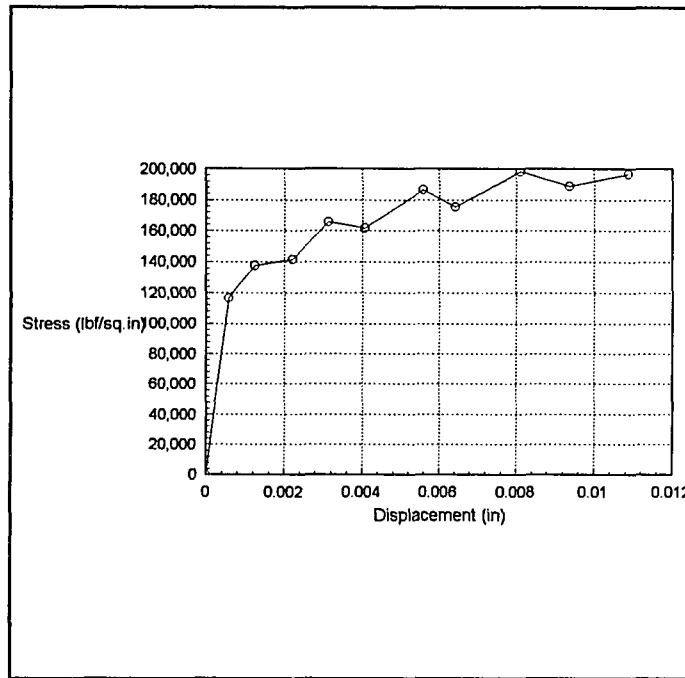


Figure 3.12 Relation between Average Contact Stress (σ_z) and Contact Node Displacement (z)

From regression analysis, the following relation are obtained.

$$\sigma_z = 33000 z^{1.25} \quad (3.11)$$

$$a = -3.5 \times 10^7 z^4 + 858108 z^4 - 7370.7 z^2 + 34.6 z - 0.0004 \quad (3.12)$$

Where,

- a - gap height
- z - contact node displacement
- σ_z - average contact stress

3.3.5 FEM determination of the Permanent Indentation

Equations, 3.11 and 3.12 are substituted in 2.17, and MathCad is used to solve for α_p . The permanent indentation and coefficient of restitution for different impact velocities are evaluated (Table 3.2).

A graph for the variation of coefficient of restitution with impact velocity is given below.

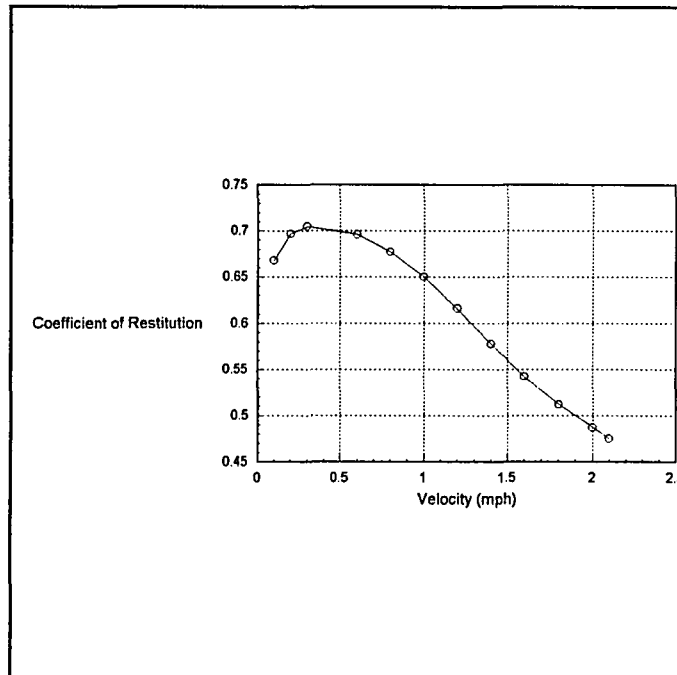


Figure 3.13 FEM Variation of Coefficient of Restitution with Impact Velocity

3.4 Comparison of Results

Coefficient restitution is used as a check to see the accuracy of the FEM analysis. It is seen from figure 3.13 that, as the velocity increases, the coefficient of restitution decreases, which indicates that the permanent indentation evaluated from the FEM analysis have the right trend. The following graphs show the Theoretical and FEM values for the Maximum Compression, Force, Coefficient of Restitution, and Permanent Indentation.

Where, theoretical values are represented by α_{mt} , F_{mt} , e_t , and α_{pt} , and the FEM values are represented by α_{mf} , F_{mf} , e_f , and α_{pf} .

It is seen that the FEM values are not far off for the Maximum Compression, Force, and the Permanent Indentation. However, it is clear that

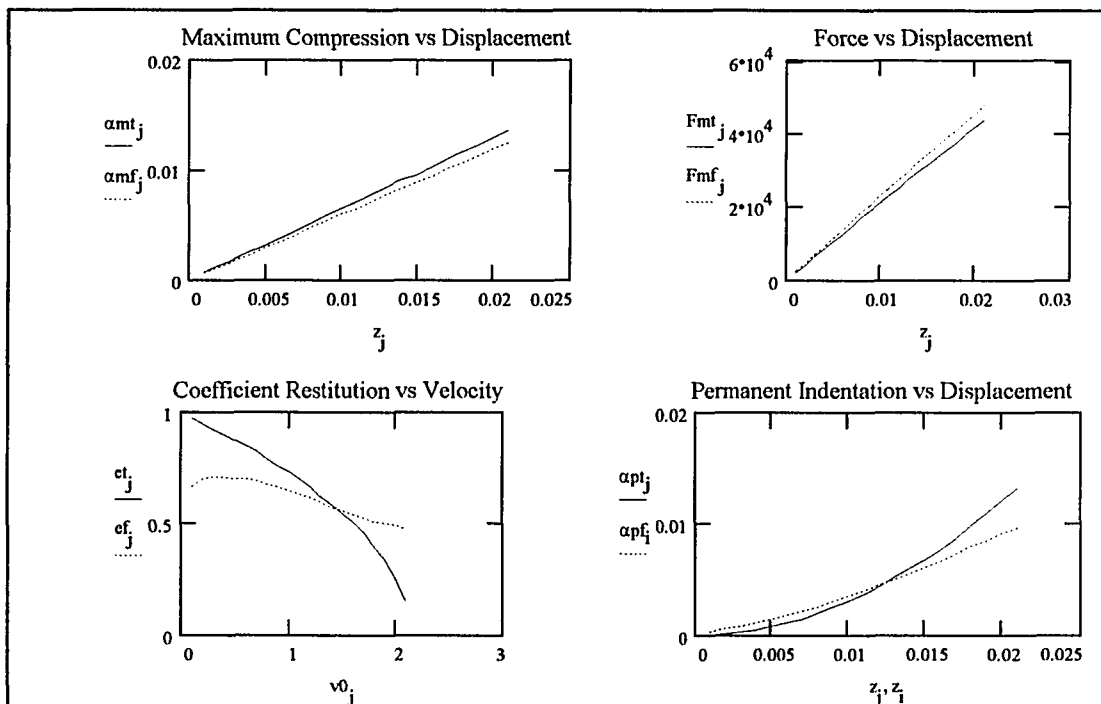


Figure 3.14 Comparison of Theoretical and FEM values for Maximum Compression, Force, Coefficient of Restitution, and Permanent Indentation

Coefficient of Restitution is only valid for a range of velocities. At low velocities (0.05 mph to 0.3 mph) FEM analysis does not hold good. The reason being that, low velocities produce small forces and only a few elements are in contact. Larger the number of elements in contact, higher will be the accuracy. From 0.05 mph to 03 mph, the coefficient of restitution is increasing, which is

theoretically inadmissible. The correct trend is for the coefficient of restitution to decrease with the increase of velocity.

The results of the two analyses for α_p , coefficient of restitution (e), compression time (τ_1), and restitution time (τ_2), are given below.

Table 3.1 - (Theoretical Results)

v (mph)	α_p (in)	e	$\tau_1 \times 10^{-4}$ (sec)	$\tau_2 \times 10^{-4}$ (sec)
0.08	1.209×10^{-6}	0.995	1.352168	1.345407
0.1	3.024×10^{-5}	0.976	5.691030	5.554445
0.2	1.209×10^{-4}	0.952	5.758144	5.481753
0.3	2.772×10^{-4}	0.927	5.862389	5.434435
0.5	7.562×10^{-4}	0.875	5.759206	5.039306
0.8	1.930×10^{-3}	0.792	5.776613	4.575077
1.0	3.020×10^{-3}	0.730	5.770379	4.212377
1.3	5.110×10^{-3}	0.628	5.792785	3.637869
1.5	6.860×10^{-3}	0.549	5.796688	3.182382
1.8	9.800×10^{-3}	0.402	5.795776	2.518966
2.0	1.210×10^{-2}	0.262	5.797582	1.518966
2.1	1.334×10^{-2}	0.148	5.797645	0.085787

Table 3.2- (FEM Results)

v (mph)	α_p (in)	e	$\tau_1 \times 10^{-4}$ (sec)	$\tau_2 \times 10^{-4}$ (sec)
0.4	0.00119	0.705	5.278953	3.721662
0.6	0.00184	0.696	5.308532	3.694738
0.8	0.00258	0.677	5.313753	3.597411
1.0	0.00343	0.650	5.300897	3.445583
1.2	0.00443	0.616	5.309543	3.270679
1.4	0.00555	0.578	5.313158	3.071006
1.6	0.00673	0.542	5.315602	2.881057
1.8	0.00791	0.512	5.315445	2.721508
2.0	0.00908	0.487	5.317515	2.586805
2.1	0.00967	0.474	5.310675	2.512520

CHAPTER 4

IMPACT ANALYSIS OF THE MPC OVERPACK

4.1 Objective

The objective of the theoretical impact analysis between solid sphere and solid cylinder (figure 4.1) is to formulate a basis to compare FEM permanent indentation of the MPC Overpack, although the latter is a hollow cylinder.

The equations derived in this section assumes that the impacting bodies are both solid. In section 4.2, FEM analysis is performed on a hollow built in cylinder in contact with a solid sphere.

4.1.1 Force Displacement Relation

The theoretical derivations in this chapter are mostly based on the equations derived by Johnson (1985). The equation for the separation h , between the surfaces using the principal relative radii of curvature R' and R'' is as follows,

$$h = \frac{1}{2R'} x^2 + \frac{1}{2R''} y^2 \quad (4.1)$$

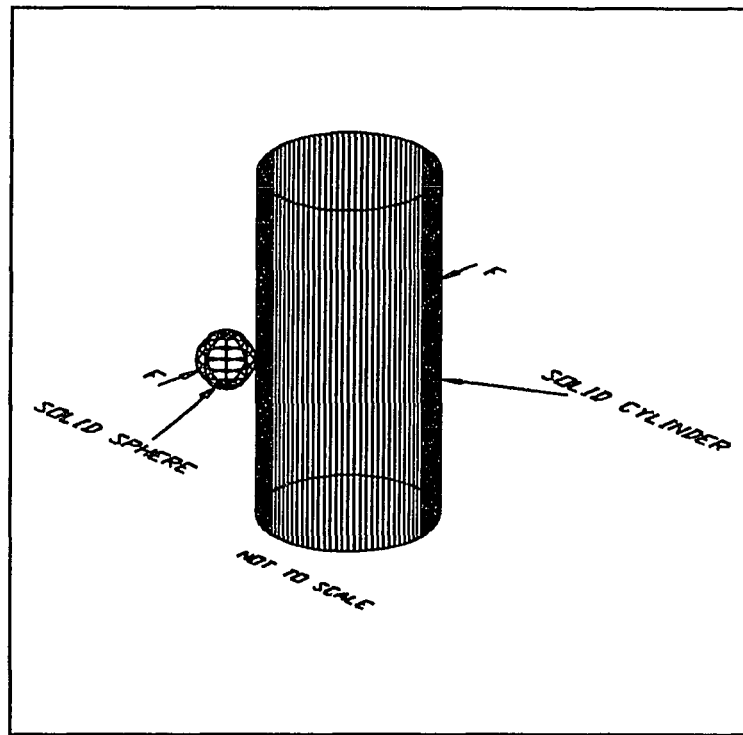


Figure 4.1 Contact of Solid Sphere and Solid Cylinder due to an Impacting Force

h is also, expressed using two positive constants A and B as follows,

$$h = A x^2 + B y^2 \quad (4.2)$$

The factors $(A+B)$ and $(B-A)$ are expressed as follows,

$$(A+B) = \frac{1}{2} \left(\frac{1}{R_1'} + \frac{1}{R_1''} + \frac{1}{R_2'} + \frac{1}{R_2''} \right) \quad (4.3)$$

$$(B-A) = \frac{1}{2} \left[\left(\frac{1}{R_1'} - \frac{1}{R_1''} \right)^2 + \left(\frac{1}{R_2'} - \frac{1}{R_2''} \right)^2 + 2 \left(\frac{1}{R_1'} - \frac{1}{R_1''} \right) \left(\frac{1}{R_2'} - \frac{1}{R_2''} \right) \cos 2\alpha \right]^{0.5} \quad (4.4)$$

Where α is the angle between the axes of the bodies. In this problem $\alpha = 0$, and

for the Sphere, $R1' = R1$, $R1'' = R1$, and for the Cylinder, $R2' = R2$, and $R2'' = \infty$.

The following relation between a , b , A and B is given by,

$$\frac{b}{a} = \left(\frac{B}{A} \right)^{-\frac{2}{3}} \quad (4.5)$$

Solving for b/a ,

$$b/a = 0.9574$$

The constants A and B can also be defined as,

$$A = \rho_0 \Delta \left[\frac{b}{e^2 a^2} (K(e) - E(e)) \right] \quad (4.6)$$

$$B = \frac{\rho_0 \Delta b}{a^2 e^2} \left(\frac{a^2 E(e)}{b^2} - K(e) \right) \quad (4.7)$$

Where, $E(e)$ and $K(e)$ are complete elliptic integrals of argument (e) given by,

$$e = \left(1 - \frac{b^2}{a^2} \right)^{\frac{1}{2}} \quad (4.8)$$

The equivalent radius Re is defined as follows,

$$Re = \left(\frac{1}{R1'R1''} \right)^{0.5} \quad (4.9)$$

Using the equation for Force-Displacement given in Johnson(1985) and compensating for the FEM force we get,

$$F = \left(\frac{4}{3} \frac{\sqrt{R\theta}}{\Delta F2(\theta)^{\frac{3}{2}}} \right) \frac{1}{\delta^{1.5}} \quad (4.10)$$

Where, δ is the relative displacement, and $F2(\theta)$ is defined as follows,

$$F2(\theta) = \frac{2}{\pi} \left(\frac{b}{a} \right)^{\frac{1}{2}} \left[F1(\theta)^{\frac{1}{3}} K(\theta) \right] \quad (4.11)$$

$F1(\theta)$ is expressed as follows,

$$F1(\theta) = \left(\frac{4}{\pi \theta^2} \right)^{\frac{1}{3}} \left(\frac{b}{a} \right)^{\frac{1}{2}} \left[\left(\frac{a^2 E(\theta)}{b^2} - K(\theta) \right) (K(\theta) - E(\theta)) \right]^{\frac{1}{6}} \quad (4.12)$$

Equation 4.10 is of the form $F = K \alpha^n$.

Therefore, $n = 1.5$ and $K = 3.085 \times 10^7 \text{ lbf/in}^{1.5}$

Using, Tresca's maximum shear stress failure criterion,

$$\tau_{\max} = 0.5 Yd \quad (4.13)$$

From Table 4.1 (Johnson)

$$\tau_{\max} = 0.3114 p_0 \quad (4.14)$$

From equations 4.13 and 4.14, we get,

$$p_0 = 1.6056 Yd \quad (4.15)$$

4.1.2 Theoretical Minimum Force required to produce Plastic Deformation

Using, equation for the maximum contact pressure given in Johnson, the minimum force to produce plastic deformation (F_p), is as follows,

$$F_p = \frac{\rho_0^3 \pi^3 R e^2 \Delta^2}{6} F1(e)^{-2} \quad (4.16)$$

Substituting for ρ_0 ,

$$F_p = 384.5 \text{ lbf}$$

4.1.3 Theoretical Minimum Velocity required to produce Plastic Deformation

Referring to equation 2.12 in chapter 2 and using MathCad,

$$V_p = 0.004 \text{ mph}$$

4.1.4 Determination of Permanent Indentation

In this problem, it is reasonable to assume that the area of contact is elliptical. Johnson derived the equation for the pressure at a point for an elliptical region within the contact boundary in terms of the maximum pressure ρ_0 . Pressure at a point is given by,

$$\rho(x,y) = \rho_0 \sqrt{1 - \frac{x^2}{a^2} - \frac{y^2}{b^2}} \quad (4.17)$$

Where, a and b are the semi major and minor axes of the ellipse.

Total Force (F) on the elliptical region is given by,

$$F = 4 \int_0^b \int_0^{a\sqrt{1-\frac{y^2}{b^2}}} \rho_0 \sqrt{1-\frac{x^2}{a^2}-\frac{y^2}{b^2}} dx dy \quad (4.18)$$

This integral reduces to,

$$F = \frac{2}{3} a b \pi \rho_0 \quad (4.19)$$

From equation 4.5,

$$a = 1.0444 b$$

Then, equation 4.19 reduces to,

$$F = 1.1180 b^2 \pi Yd \quad (4.20)$$

Substituting, for b in the above equation,

$$F = 2.2360 \pi Yd R z \quad (4.21)$$

Integrating with respect to z gives the energy absorbed during the impact.

$$E = 2.2360 \pi Yd R \int_0^z z dz \quad (4.22)$$

The above equation reduces to,

$$E = 3.5123 R Yd z^2 \quad (4.23)$$

The above expression is substituted in equation 2.17 to evaluate the permanent

indentation. The expression for energy is as follows,

$$\frac{F_m \alpha_p}{n+1} = \sum_{l=1}^2 3.5123 Y_d R_l z_l^2 \quad (4.24)$$

The above equation is solved for different impact velocities. Permanent indentation α_p , and the coefficient of restitution are tabulated (Table 4.1).

The following graph (figure 4.2) shows the theoretical variation of coefficient of restitution with impact velocity.

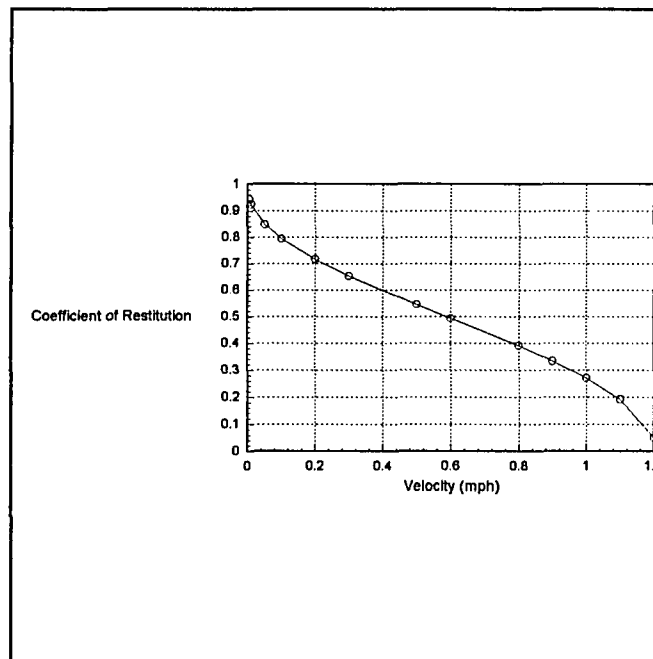


Figure 4.2 Theoretical variation of Coefficient of Restitution with Impact Velocity

4.2 FEM Modeling of Multi Purpose Overpack

4.2.1 Multi Purpose Canister Overpack

Multi Purpose Canister (MPC) Overpack (figure 4.3, and figure 4.4) is an

outer casing for the nuclear canister, which will be used in transporting nuclear waste. The canister is lowered into the Overpack and is closed using a lid. The Overpack consists of two layers which are fused together. The diameter of the outer carbon steel sleeve is 59.212 inches, and has a thickness of 3.937 inches. Alloy 825 (Inconel) is the inner sleeve and has a thickness of 0.374 inches. The overall length of the Overpack is 220.47 inches.

4.2.2 FEM Modeling of MPC Overpack

In end closed hollow cylinders, the sectional plane at half length is weak compared to a plane close to the ends. Therefore, the impact is made to take place on a plane half way along the length of the Overpack. Taking advantage of the geometric symmetry, only one quarter of the Overpack is considered for analysis. Therefore, only a quarter of the cross-section of the Overpack (figure 4.5), is modeled. In generating the two layers of the Overpack, two different element groups defining the respective material properties were declared. The material properties are declared in the same manner discussed in chapter three. Section 3.2.2 describes how ETAN is defined for the two bodies. Eight node solid elements were meshed using the M_VL command in such a way that closer to the contact region has a higher element density. The smallest element size was about quarter inch in length. The COSMOS/M code source file is given in Appendix IV.

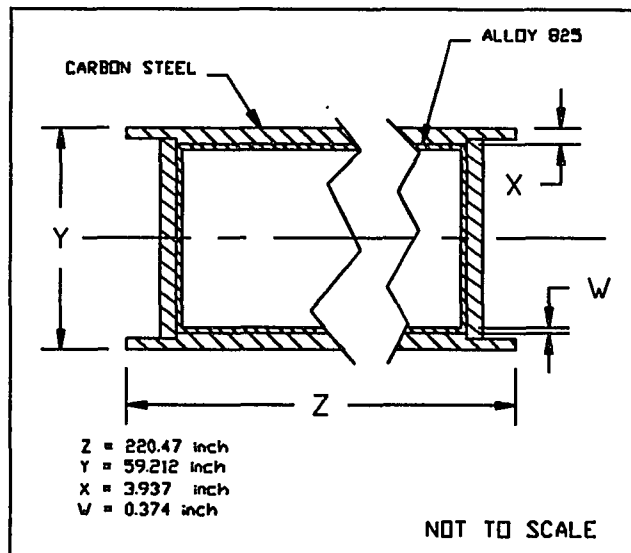


Figure 4.3 MPC Overpack - Sectional View

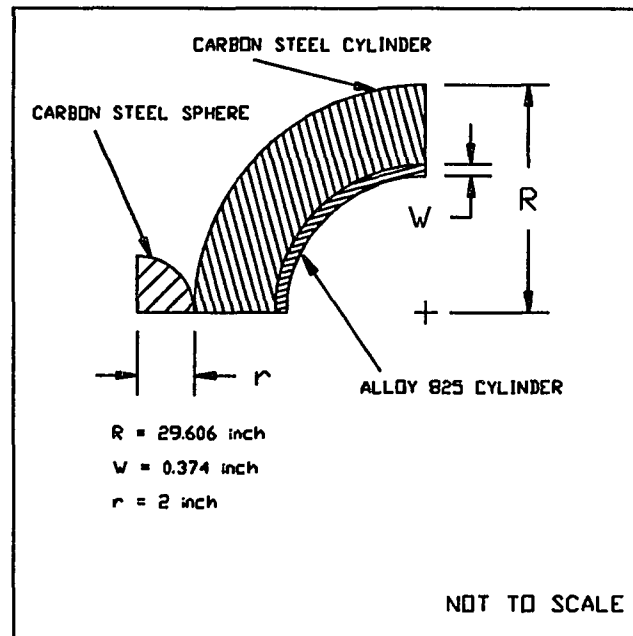


Figure 4.4 Sphere in contact with MPC Overpack

4.2.3 Impacting Object

A moving carbon steel sphere is modeled as the impacting object (figure 4.6 and figure 4.7). The size of the sphere was chosen about fifteen times smaller than the diameter of the Overpack. Larger curvature of the impacting body produces better indentation. Also, soft materials disintegrate easily on impact with tough materials therefore, steel was chosen as the material for the sphere. The sphere is allowed to impact with the stationary Overpack. The material properties of the sphere are the same as that for the carbon steel outer layer ($E = 30 \times 10^6$ lbf/in², $\nu = 0.3$). Also, the tangent modulus is defined using the ETAN command. Since, the program did not accept zero for the tangent modulus, 1×10^6 lbf/in² had to be used in order to make the program run without crashing. Eight node solid elements were created using the PHSWEEP command to form the sphere. Taking advantage of geometric and loading symmetry, an eighth of the sphere was modeled.

4.2.4 Boundary Conditions

For structural stability and problem definition requirements, the boundary conditions are applied in such a way that the Overpack is held stationary, resting on the ground. The motion of the common boundary of the outer carbon steel sleeve is restricted, and is prevented from moving into the inner inconel sleeve. In addition to the above conditions, all the nodes in the model are only allowed to move along the direction of the force. The source file containing the geometry, material properties, boundary conditions, force and solution technique etc., is given in Appendix IV.

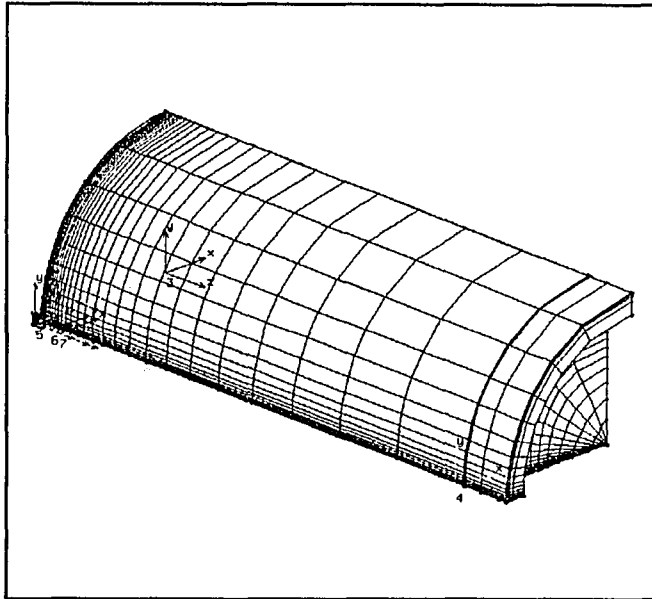


Figure 4.5 FEM Model of Sphere and Cylinder in contact

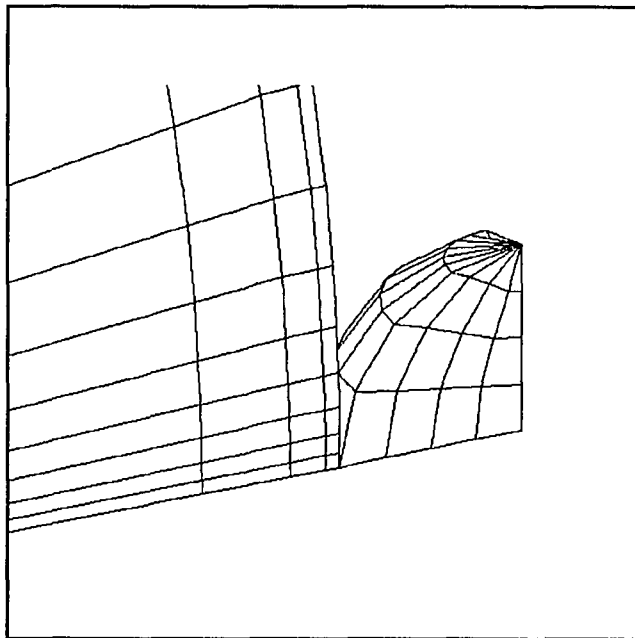


Figure 4.6 Sphere in contact with Cylinder

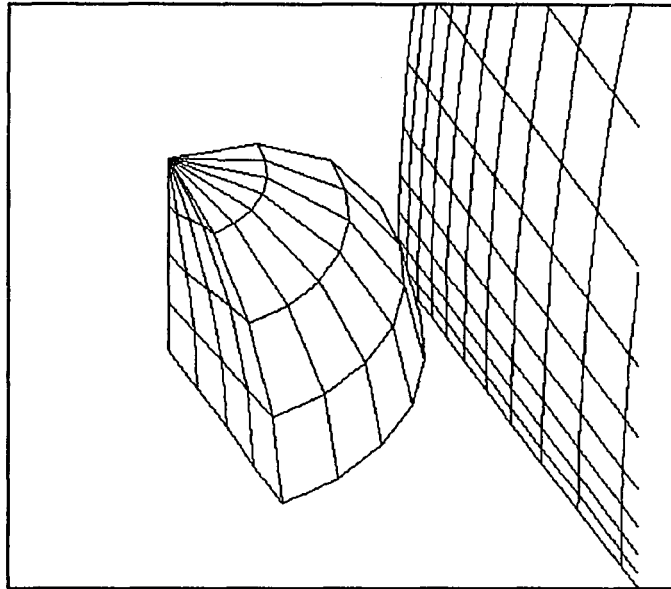


Figure 4.7 Close up view of the contact region

4.2.5 Gap Surfaces and Gap Elements

In the 2D model, gap lines were created to facilitate nonlinear analysis, but for 3D analysis four node gap surfaces (figure 4.8) instead of lines are created on the sphere surface and one node gap elements are created on the cylinder surface. In declaring the gap surfaces, the same command `NL_GS` is used as in the 2D analysis, but only the number of nodes differ. A three by three element grid containing the point of contact was declared for analysis.

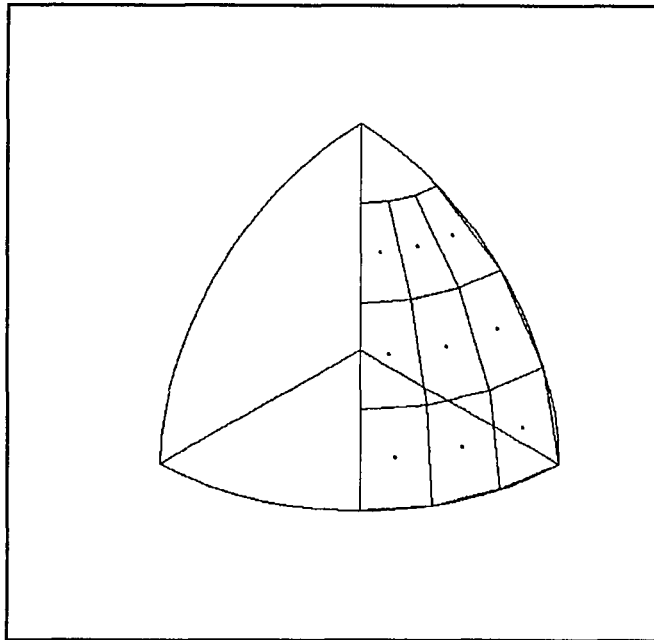


Figure 4.8 Three by three Gap Surface on Sphere

4.2.6 Non-linear Static Analysis

Non linear static analysis is performed on the system using NSTAR module of COSMOS/M. The nodal displacements around the point of contact are written into the output file. It was observed that the effect of the static loading is concentrated around the point of contact. The effective area was found to be a five by five element grid on the MPC Overpack and a three by three element grid on the sphere. Therefore, only the effective area was considered in the analysis. Since, COSMOS/M program does not give strain energy for the elements in the output file, a separate Fortran program (Appendix V) was written to calculate the volume of the indentation caused by the impact and the average contact stress of the respective elements. This program also calculates the product of, average stress and volume.

The data obtained from the Fortran program is used in the following section to evaluate the permanent indentation.

4.3 FEM determination of the Permanent Indentation

4.3.1 Elastic Analysis

The model was subjected to an impact load (682.5 lbf) such that no plastic stresses are developed. COSMOS/M (Appendix IV) was used to analyze the resulting nodal displacements. The purpose of this analysis is to determine the power index (n), and the stiffness K .

The value of the load (F) and the corresponding displacement of the contact node (z) is tabulated (Table 4.3.1-Appendix VI), and a graph of Force versus Displacement is plotted (figure 4.9).

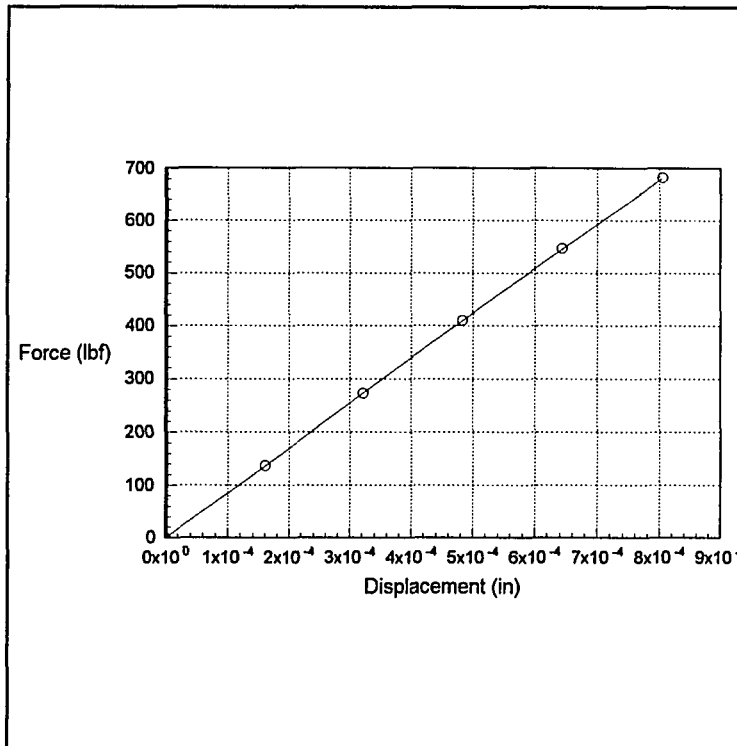


Figure 4.9 Relation between Applied Load (F) and Contact Node Displacement (z)

From regression analysis,

$$n = 1 \quad K = 847751 \text{ lbf/in}$$

4.3.2 FEM Minimum Force required to produce Plastic Deformation

The minimum force required to produce plastic deformation was found by performing several trials with different loads, and checking the stress at the contact node for yield. This force (F_p) was found to be 887.2 lbf.

4.3.3 FEM Minimum Velocity required to produce Plastic Deformation

Referring to equation 2.12 in chapter 2, and using MathCad,

$$V_p = 0.05 \text{ mph}$$

4.3.4 Plastic Analysis

For plastic analysis a load of 2100 lbf is used, and the results of the analysis is written into COSMOS/M output file. The edited output file is the input file to the Fortran program (Appendix V) which calculates the product of stress and volume, corresponding to the respective contact node displacement. Output from the Fortran program is given in Appendix F (Table 4.3.4).

A plot of Energy versus Contact Node Displacement (z) is given below (figure 4.10).

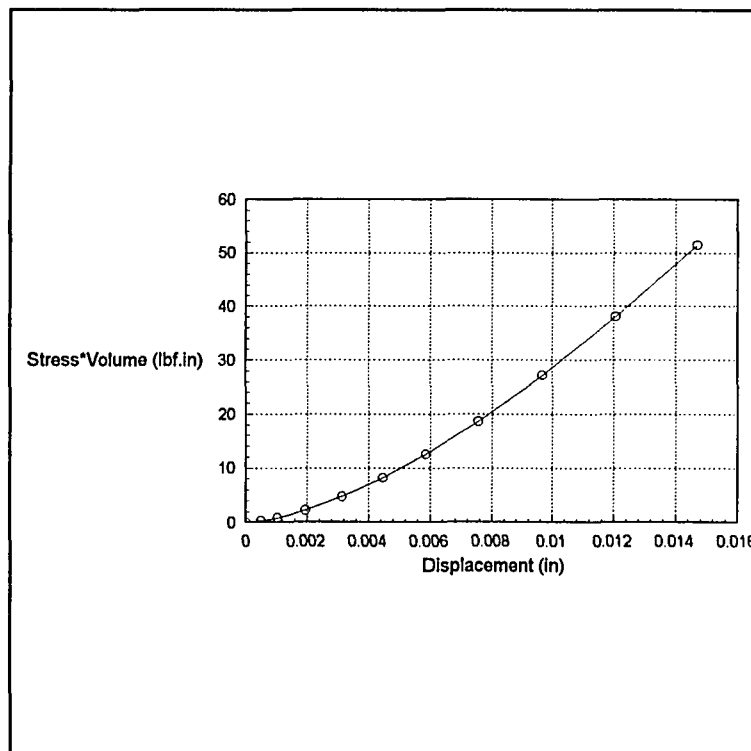


Figure 4.10 Relation between Energy Absorbed during Impact and Contact Node Displacement (z)

A curve fit of the data for the above graph (Appendix VII) yields the following relation.

$$\sigma_z = 4.18 \times 10^8 z^4 - 1.03 \times 10^7 z^3 + 2.05 \times 10^5 z^2 + 2087.9 z \quad (4.25)$$

Where, σ_z - Average contact stress
 z - Contact node displacement

Substituting the above relation in equation 2.17, the permanent indentation and the coefficient of restitution for different impact velocities are evaluated and tabulated (Table 4.2).

The following graph (figure 4.11) shows the variation of the Coefficient of Restitution with Impact Velocity.

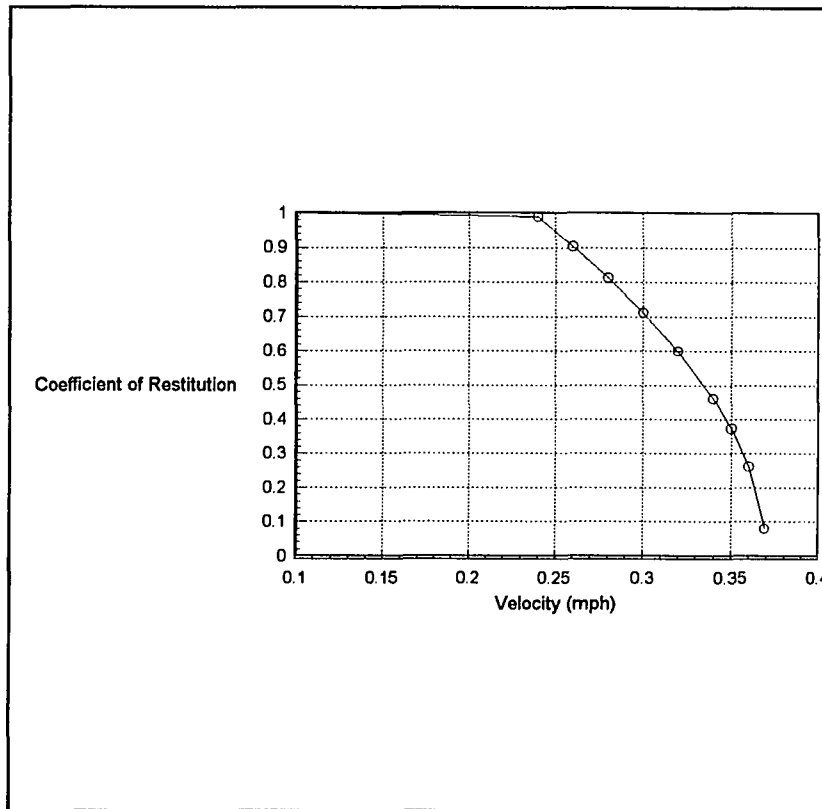


Figure 4.11 Relation between FEM Coefficient of Restitution and Impact Velocity

It is seen from the graph that as the velocity increases the coefficient of restitution decreases, which is the right trend. Another important observation is that, before 0.24 mph, the graph lost its smooth trend. This is due the fact that at low velocities fewer elements are in contact, and the results lose accuracy.

4.4 Comparison of Results

The theoretical analysis is performed for the impact of a solid sphere and solid cylinder. The FEM analysis is performed for the impact of a solid sphere and hollow cylinder. The FEM model is 4.3 inch thick, and has a diameter of 29.606 inches. This resembles a thick shell and will with stand high velocity impact as a

solid cylinder which has the same dimensions and approximate mass. A thin shell on the other hand, will deform making the body out of shape. In this instance the deformation is local and only a small region is affected unlike in a thin cylinder, where the deformation is spread over a large area. The valid velocity range for the FEM model is from 0.24 mph to about 0.37 mph, where as for the solid model it varies from 0.004 mph to 1.2 mph. The energy absorbed in the bodies was observed to be close. However, the accuracy of the FEM analysis is difficult to predict in this case. The only observation that can be made is, how close is the FEM analysis, compared to the Theoretical analysis.

The following graphs show Theoretical and FEM values for the Maximum Compression, Force, Coefficient of Restitution, and Permanent Indentation.

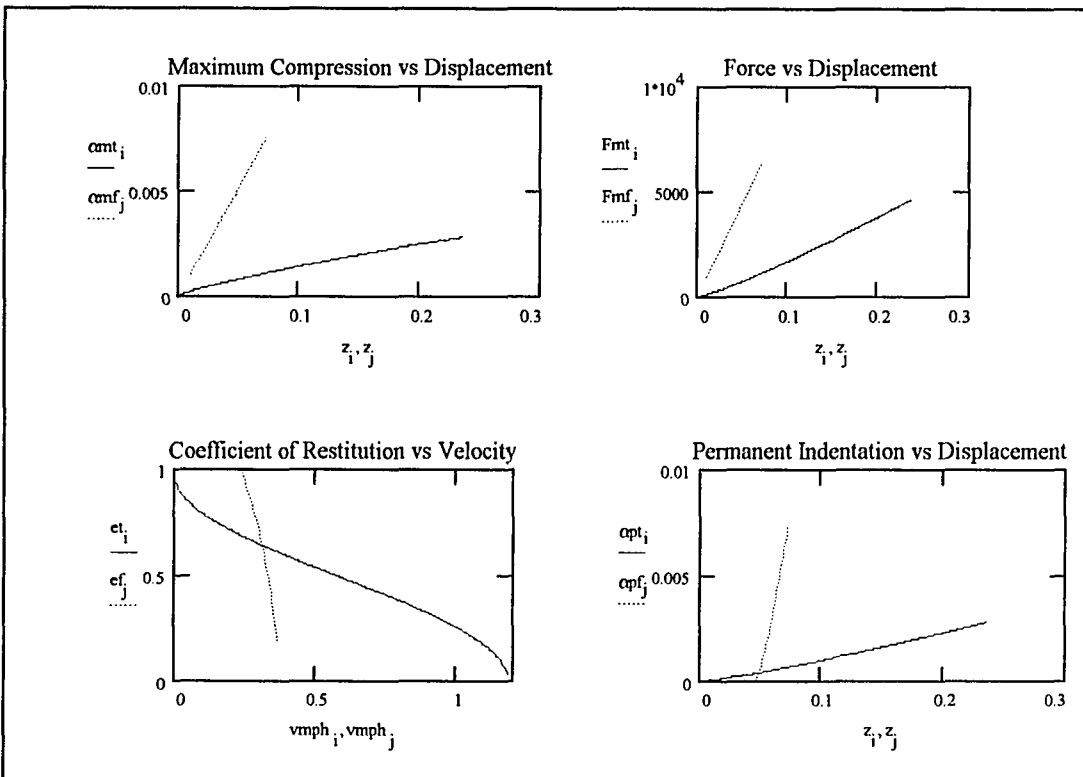


Figure 4.12 Comparison of Theoretical and FEM values for Maximum Compression, Force, Coefficient of Restitution, and Permanent Indentation

Where, theoretical values are represented by α_{mt} , F_{mt} , e_t , and α_{pt} , and the FEM values are given by α_{mf} , F_{mf} , e_f , and α_{pf} .

It is seen that the FEM values are close around 0.3 mph. The following tables give the Theoretical and FEM results.

Table 4.1 - (Theoretical Results)

v (mph)	α_p (inch)	e	$\tau_1 \times 10^{-4}$ (sec)	$\tau_2 \times 10^{-4}$ (sec)
0.005	3.980×10^{-6}	0.942	5.956875	5.612992
0.01	9.143×10^{-6}	0.923	5.185760	4.786798
0.05	6.308×10^{-5}	0.848	3.758534	3.185577
0.1	1.449×10^{-4}	0.794	3.271993	2.593697
0.2	3.329×10^{-4}	0.716	2.848436	2.033448
0.3	5.415×10^{-4}	0.653	2.626565	1.708850
0.5	9.997×10^{-4}	0.545	2.371474	1.282659
0.6	0.001244	0.494	2.286558	1.117886
0.8	0.001757	0.390	2.158710	0.825442
0.9	0.002024	0.333	2.108453	0.683299
1.0	0.002296	0.270	2.064488	0.532386
1.1	0.002575	0.192	2.025507	0.352143
1.2	0.002858	0.05	1.990564	0.012779

Table 4.2 - (FEM Results)

v (mph)	α_p (inch)	e	τ_1 (sec)	τ_2 (sec)
0.1	1.963×10^{-7}	0.999	0.000342	0.000134
0.24	1.041×10^{-4}	0.989	0.001841	0.001821
0.26	9.843×10^{-4}	0.903	0.001830	0.00165
0.28	0.001969	0.812	0.001842	0.00149
0.30	0.003053	0.712	0.001845	0.00131
0.32	0.004243	0.599	0.001846	0.00110
0.34	0.005544	0.460	0.001847	0.00084
0.35	0.006231	0.373	0.001845	0.00068
0.36	0.006938	0.262	0.001846	0.00048
0.369	0.007587	0.08	0.001824	0.00032

CHAPTER 5

CONCLUSIONS AND RECOMMENDATIONS

5.1 Conclusions

Preliminary study of FEM analysis for the static loading of plane cylinders, yielded reasonable results within a range of velocities (0.3 mph to 2.1 mph). The Force, Maximum Compression and the Permanent Indentation were observed to be acceptable compared to theoretical values. The evaluated values for the permanent indentation were of the order of one thousandth of an inch, at the low end, and the maximum relative error was fourteen percent. Experimental data for impact of cylinders was not available for comparison, though it is concluded that COSMOS/M 1.7 Finite Element software yields acceptable results for the impact of two dimensional cylinders under plane stress conditions. It is also concluded that the FEM results have the right trend for the MPC Overpack. The theoretical model (solid sphere and solid cylinder) is no proper comparison to check the accuracy of the FEM analysis. The FEM analysis showed a deviation from the solid cylinder model. The most significant difference in this regard is the power index of the Hertz contact force. The FEM analysis yielded $n = 1$, while the theoretical value was 1.5. The stiffness was ten times lower than the theoretical value. Since, a hollow

cylinder shows much resemblance to a thick shell than a solid cylinder, the discrepancy in the results cannot be solely attributed to FEM analysis error.

FEM analysis, is an approximate solution. Interpretation of the FEM results is important, as the output of the program may be erroneous. A pre knowledge of the exact solution is an advantage in interpreting FEM results.

Accuracy of FEM results depend on several factors, the main criterion being the mesh density around the area of interest. However, there are limitations as to how fine the elements can be made. On the other hand there are convergence problems in the FEM software. Due to these reasons, the user has very little choice in controlling the software solution techniques to get the desired results.

It is concluded that the COSMOS/M 1.7 software yields reasonable results within limits for the impact analysis of the MPC Overpack.

5.2 Recommendations

The degree of damage to the MPC Overpack depends on the amount of indentation caused during the impact. Although, FEM analysis, has its limitations, it is a reasonable method of determining the permanent indentation. Since, there is no valid comparison available, it is recommended that physical measurement of the indentation be made if possible, and compared with FEM results before any decisions are made, as human safety and environment are main criteria in this issue. Future study is also necessary to ascertain the accuracy of the FEM analysis.

APPENDIX I

DESCRIPTION OF COSMOS/M 1.7 FEM SOFTWARE APPLICATIONS.

Finite Element Analysis

The finite element method is a numerical method with computer adaptation. The basis of this method is to formulate the problem into a system of simultaneous algebraic equations instead of a system of differential equations. This is because, a system or a body is modeled by subdividing it into smaller elements (finite elements) which are connected at nodes. Finite element analysis involves the following steps:

1. Divide the structure or continuum into finite elements.
2. Define material properties of each element.
3. Assemble elements to obtain the finite element model of the structure.
4. Apply the known loads (nodal forces and moments).
5. Specify how the structure is supported by declaring the boundary conditions.
6. Solve simultaneous linear algebraic equations to determine nodal degrees of freedom (nodal displacements).
7. Calculate element strains from the nodal d.o.f. and the element displacement field interpolation, and finally calculate stresses from strains.

The power of the finite element method resides principally in its versatility. This method (FEM) can be applied to a variety of problems. The system or the body under analysis can have arbitrary loading, and support conditions. The method also can generate different mesh types for different elements types, shapes, and physical properties. This great versatility is contained within a single computer

program. User-prepared input data controls the selection of analysis process, geometry, boundary conditions, and element type. Another attractive feature of finite elements is the close physical resemblance between the actual structure and its finite element model.

The finite element method also has disadvantages. A computer, a reliable program, and intelligent use of program are essential. A general purpose program has extensive documentation, which cannot be ignored. Experience and good engineering judgement are needed in order to define a good model. Interpretation of results is important as it is very easy to make erroneous problem formulation. Preknowledge of expected results is helpful.

The module GASTER is used to develop the geometric model and mesh generation of the system. GEOSTAR is an interactive full three dimensional graphic geometric modeler, mesh generator, and finite element pre and postprocessor. The geometric modeling capabilities of GEOSTAR are based on mixed boundary representation and parametric cubic equations. The primary application of GASTER is to function as a pre and postprocessor to the COSMOS/M finite element analysis system. The user can create the model, supply all related analysis information, invoke the analysis using the COSMOS/M analysis modules, and review the results, all from within GASTER in an interactive, menu driven, graphic environment. A diverse set of geometric modeling capabilities combined with flexible meshing options allow for the creation and meshing of complex models with ease. Loading, boundary and initial conditions can conveniently be applied in association with geometric entities and in any defined coordinate system.

COSMOS/M, as it is, was not fully applicable to this analysis, so some fortran programs were written to evaluate the necessary quantities for graphical representation and regression analysis.

There are two options in the SOLID element - twenty node and eight node. Eight node SOLID element is used in this analysis to make computation easier.

Nonlinear Analysis

The success of a finite element analysis depends largely on how accurately the geometry, the material behavior, and the boundary conditions of the actual problem are idealized.

While elements with their geometric characteristics and boundary conditions are used to describe the geometric domain of the problem, material models (constitutive relations) are introduced to capture the material behavior. All real structures behave nonlinearly in one way or the another.

In some cases due to the nature of the problem, a linear solution may be adequate. However, in many other situations a linear solution has proven to be catastrophic and a nonlinear analysis becomes a must.

A major part of structural nonlinearities arise from Geometrical, Material and Contact (boundary) nonlinearities. Structures undergoing large displacements can have significant changes in their geometry due to loading induced deformations which can cause the structure to respond nonlinearly in a stiffening and/or softening manner. Several factors can cause the material behavior to be nonlinear. The dependency of the material stress-strain relation on the load history (as in plasticity problems), load duration (as in creep analysis) are some of these factors. A special class of nonlinear problems is concerned with the changing nature of the boundary conditions of the structures involved in the analysis during motion. This situation is encountered in the analysis of contact problems. Pounding of structures, gear-tooth contacts, fitting problems, threaded connections, and impact bodies are several examples requiring the evaluation of the contact boundaries. The evaluation of contact boundaries (nodes, lines, or surfaces) can be achieved by using gap (contact) elements between nodes on the adjacent boundaries.

Solution Strategies to Nonlinear Problems

For nonlinear problems, the stiffness of the structure, the applied loads, and/or boundary conditions can be affected by the induced displacements. The equilibrium of the structure must be established in the current configuration which

is unknown a priori.

At each equilibrium state along the equilibrium path, the resulting set of simultaneous equations will be nonlinear. Therefore, a direct solution will not be possible and an iterative method will be required.

Several strategies have been devised to perform nonlinear analysis. As opposed to linear problems, it is extremely difficult, if not impossible to implement one single strategy of general validity for all problems. Very often, the particular problem at hand will force the analyst to try different solution procedures or to select a certain procedure to succeed in obtaining the correct solution. For these reasons, it is imperative that a computer program used for nonlinear analyses should possess several alternative algorithms for tackling wide spectrum of nonlinear applications. Such techniques would lead to increased flexibility and the analyst would have the ability to obtain improved reliability and efficiency for the solution of a particular problem.

Output options

The PRINT_OPS command along with the PRINT_NOD command is used to instruct the program to write the nodal displacements into the output file (problem_name.OUT). The PRINT_EL command writes the nodal stresses into the output file.

Tools

The commands used in the non linear analysis are explained as follows. It is generally recommended that the DATA_CHECK command be issued prior to any solution step. DATA_CHECK command checks that an element group, a material property set, and a real constant set (if needed) have been defined for each element in the database. R_CHECK command may be issued before running any analysis. The R_CHECK command performs a thorough check on the database of the current problem and prepares a report on the status of the input in a file named problem_name.CHK. It performs all functions of DATA_CHECK, namely checking that there is an element group, a material property set and a real constant set

associated with each element. It issues a warning message if a nonexistent node is issued to define the element. For solid element, the aspect ratio is checked. The A_STATIC command specifies details of the linear static analysis to be performed by the R_STATIC command. Gravity loading flag is activated in A_STATIC command. The R_STATIC command performs a linear STATIC analysis and it calculates nodal displacements using the STAR program.

Results

The ACTDIS command loads the specified displacement component corresponding to a load case or time step from the current database into the plot buffer. The DISPLOT command produces a vector or contour plot for the displacement component loaded into the plot buffer by the ACTDIS command. A contour plot connects points of equal displacements and can be colored lines or color filled. Linear interpolation is used to determine the points of equal displacements.

APPENDIX II

COSMOS/M CODE FOR PLANE CYLINDERS

TITLE, CONTACT OF TWO PLANE CYLINDERS

c* Element group and Material properties

c* 1020 HR Steel

EGROUP,1,PLANE2D,0,1,0,0,1,0,0,

RCONST,1,1,1,2,1,0,

MPROP,1,EX,30E6,

MPROP,1,NUXY,0.3,

MPROP,1,SIGYLD,1.092E5,

MPROP,1,ETAN,1E6,

MPROP,1,DENS,7.246E-4,

MPROP,1,GXY,11.5E6,

VIEW,0,0,1,0,

c* Define points, curves and surfaces

PT,1,0,0,0,

PT,2,1,0,0,

PLANE,Z,0,1,

CRPCIRCLE,1,1,2,1,90,2,

SF4COR,1,0,0,0,0.5,0,0,0.5,0.5,0,0,0.5,0,

SF2CR,2,1,6,0,

SF2CR,3,2,4,0,

c* Mesh surfaces

M_SF,2,2,1,4,20,20,5,5,

M_SF,3,3,1,4,20,20,1,5,

M_SF,1,1,1,4,20,20,1,5,

NMERGE,1,,1,0.0001,0,1,0,

c* Create the second cylinder using symmetry

ACTDMESH,SF,1,

SFSYM,1,3,1,X,1,2,

c* Merge and compress nodes

NMERGE,1,,1,0.0001,0,1,0,

NCOMPRESS,1,,1,

ECOMPRESS,1,,1,

c* Define time curve and set time increments

CURDEF,TIME,1,1,0,0,1,1,

TIMES,0,1,0.1,

ACTSET,TC,1,

c* Boundary conditions

DCR,3,UY,0,7,4,,

DCR,5,UX,0,9,4,,

DCR,15,UY,0,12,3,

SCALE,0,

c* Gap element group

EGROUP,2,GAP,1,0,0,1,2,0,0,

c* Define gap lines and point elements

NL_GS,1,10,9,

NL_GS,2,9,8,

NL_GS,3,8,7,

NL_GS,4,7,6,

NL_GS,5,6,5,

NL_GS,6,5,4,

NL_GS,7,4,3,

NL_GS,8,3,2,

NL_GS,9,2,1,

EL,,PT,0,1,1720,0,0,0,0,0,0,

EL,,PT,0,1,1718,0,0,0,0,0,0,

EL,,PT,0,1,1716,0,0,0,0,0,0,

EL,,PT,0,1,1714,0,0,0,0,0,0,

EL,,PT,0,1,1712,0,0,0,0,0,0,

EL,,PT,0,1,1710,0,0,0,0,0,0,

EL,,PT,0,1,1708,0,0,0,0,0,0,

EL,,PT,0,1,1706,0,0,0,0,0,0,

EL,,PT,0,1,1703,0,0,0,0,0,0,

c* Plot gap lines

NL_GSPLOT;

c* Force on cylinder

FCR,11,FX,-21.0,18,7,

c* Non linear solution

NL_SOL,1,0,

c* Print nodal displacements and stresses

PRINT_OPS,1,0,0,0,0,0,0,0,1,0,

PRINT_NDSET,1,1,7,

PRINT_ELSET,1,1,6,

c* Run non linear analysis

R_NONLINEAR

APPENDIX III

MATHCAD CALCULATIONS FOR PLANE CYLINDERS

Evaluation of F_p , V , and α_p

$$D = 2 \text{ in} \quad R = D/2 \quad \rho = 0.2799 \text{ lbm/in}^3 \quad E = 30 \times 10^6 \text{ psi}$$

$$Y_d = 2.6 \times 42000 \text{ psi} \quad F_m = 24600 \text{ lbf} \quad n = 1$$

$$V = \pi \cdot 1^2 \cdot 1 \cdot 1/4 \quad m = \rho \cdot V \quad K = 3843860 \text{ lbf/in}$$

$$m_1 = m \quad m_2 = m \quad z_1 = z_2$$

$$z = z_1$$

$$z = \alpha/2$$

$$K_d = D^2 / (2 \cdot D)$$

$$F_p = Y_d^2 \cdot K_d / (0.591^2 \cdot E)$$

$$F_p = 1138.18 \text{ lbf}$$

Tresca's Failure Criterion

$$\tau_{\max} = 0.5 Y_d$$

Johnson Chapter 4

$$\tau_{\max} = 0.3 p_0$$

From Geometry

$$a = \sqrt{2Rz}$$

Minimum Velocity to produce plastic deformation

$$V_p = \sqrt{\left(\frac{F_p}{2}\right)^{\frac{n+1}{n}} K^{-\frac{1}{n}} \left(\frac{2}{n+1}\right) \left(\frac{m_1+m_2}{m_1 m_2}\right)}$$

$$V_p = 0.8753 \text{ in/sec}$$

Maximum Displacement

$$\alpha_m = \left(\frac{F_m}{K}\right)^{\frac{1}{n}}$$

$$\alpha_m = 0.0064 \text{ in}$$

Initial Velocity corresponding to F_m

$$V_0 = \sqrt{2 K \left(\frac{\alpha_m^{n+1}}{n+1}\right) \left(\frac{m_1+m_2}{m_1 m_2}\right)}$$

$$V_0 = 37.84 \text{ in/sec}$$

Time of duration of the Compression Phase

$$\tau_1 = \frac{\alpha_m}{V_0} \int_0^1 \frac{1}{\sqrt{1-u^{n+1}}} du$$

$$\tau_1 = 2.6562 \times 10^{-4} \text{ sec}$$

Theoretical determination of α_p

Guess value $\alpha_{pr} = \alpha_m/2$

$$\alpha_p = \text{root} \left(\sum_{i=1}^2 \int_0^a \int_0^a \frac{p_0}{a} \sqrt{a^2 - y^2} dy dz - \frac{F_m \alpha_{pr}}{n+1}, \alpha_{pr} \right)$$

$$\alpha_p = 0.00458 \text{ in}$$

Determination of α_p using FEM

Guess value $\alpha_{p1} = \alpha_m$

$$f(z) = -0.0004 + 34.57 z - 7370.69 z^2 + 858108 z^3 - 3.4952 \cdot 10^7 z^4$$

$$\sigma_z = 33000 z^{1.25}$$

$$\alpha p2 = \text{root} \left(2 \int_0^{\alpha p1} 33000 z^{1.25} f(z) dz - \frac{F_m \alpha p1}{n+1}, \alpha p1 \right)$$

$$\alpha p2 = 0.005804 \text{ in}$$

Time of duration of the Restitution Phase

$$\tau_2 = \frac{(\alpha_m - \alpha p2)}{V_0 e} \int_0^1 \frac{1}{\sqrt{1-u^{n+1}}} du$$

$$\tau_2 = 8.1077 \times 10^{-5} \text{ sec}$$

APPENDIX IV

COSMOS/M CODE FOR SPHERE AND CYLINDER

TITLE CONTACT OF BUILT IN TWO HOLLOW CYLINDERS AND SPHERE (3D)

SUBTITLE 8 NODE SOLID ELEMENTS - 21000 LBF LOAD

c* Element group of cylinder and material properties

c* 1020 HR Steel

EGROUP 1 SOLID 0 2 0 0 1 0 0

MPROP 1 EX 30E6

MPROP 1 NUXY 0.3

MPROP 1 SIGYLD 1.092E5

MPROP 1 ETAN 1E6

MPROP 1 DENS 7.246E-4

MPROP 1 GXY 11.5E6

ACTSET EG 1

ACTSET MP 1

VIEW 0 0 1 0

c* Define points for cylinder

ACTSET CS 0

PT 1 0 0 0

PT 2 31.606 0 0

PT 3 2 0 0

PTGEN 1 3 3 1 0 3.937 0 0

c* Change coordinate system

CSANGL 3 0 31.606 0 0 0 0 0

ACTSET CS 3

PTGEN 1 4 4 1 1 0 0 -90

PTGEN 1 3 3 1 1 0 0 -90

c* Activate global coordinate system

ACTSET CS 0

PLANE Z 0 1

c* Curves, surfaces and volume for Steel cylinder

CRARC 1 6 3 2 29.606

CRLINE 2 3 4

CRARC 3 4 5 2 25.669

CRLINE 4 5 6

SF4CR 1 1 2 3 4 0

CSANGL 4 0 0 0 99.9252 0 0 0

ACTSET CS 0

SFCOPY 1 1 1 4

VIEW 1 1 -3 0

VL2SF 1 2 1 1

c* Generate quadrilateral mesh for Steel cylinder

M_VL 1 1 1 8 16 4 28 80 16 0.01

c* Element group of Sphere and material properties

EGROUP 2 SOLID 0 2 0 0 1 0 0

MPROP 2 EX 30E6

MPROP 2 NUXY 0.3

MPROP 2 SIGYLD 1.092E5

MPROP 2 ETAN 1E6

MPROP 2 DENS 7.246E-4

MPROP 2 GXY 11.5E6

ACTSET EG 2

ACTSET MP 2

c* Points, curves and surfaces for Sphere

ACTSET CS 0

PT 11 0 2 0

CRLINE 13 3 1

CRLINE 14 1 11

CRARC 15 11 3 1 2

SF3CR 7 13 14 15 0

c* Generate quadrilateral mesh for Sphere

M_SF 7 7 1 4 4 4 1 1

c* Generate solid elements

ACTDMESH PH 1

PHSWEEP SF 7 7 1 Y -90 1 6 1 1

c* Element group and material properties for the second Cylinder

c* Inconel 825

EGROUP 3 SOLID 0 2 0 0 1 0 0

MPROP 3 EX 28E6

MPROP 3 NUXY 0.3

MPROP 3 SIGYLD 9.36E4

MPROP 3 ETAN 1E6

MPROP 3 DENS 7.6086E-4

MPROP 3 GXY 10.76E6

c* Define points for second Cylinder

PT 13 6.311 0 0

c* Activate local coordinate system

ACTSET CS 3

PTGEN 1 13 13 1 1 0 0 -90

c* Activate global coordinate system

ACTSET CS 0

c* Create curves, surfaces and volume for Inconel Cylinder

CRLINE 21 13 4

CRLINE 22 5 14

CRARC 23 14 13 2 25.295

SF4CR 13 21 3 22 23 0

SFCOPY 13 13 1 4

VL2SF 3 14 13 1

c* Generate quadrilateral mesh for second Cylinder

ACTSET EG 3

ACTSET MP 3

M_VL 3 3 1 8 1 16 28 1 80 0.01

c* Create Inconel base

c* Create surfaces and volumes

CSANGL 5 0 0 0 0.374 0 0 0

ACTSET CS 0

SFCOPY 2 2 1 5

SFCOPY 14 14 1 5

VL2SF 4 18 2 1

VL2SF 5 19 14 1

c* Mesh volumes

ACTSET EG 1

ACTSET MP 1

M_VL 4 4 1 8 16 4 1 80 16 1

ACTSET EG 3

ACTSET MP 3

M_VL 5 5 1 8 1 16 1 1 80 1

c* Create point, curves, surface and volume for the disc

PT 23 31.606 0 99.9252

CRLINE 42 15 23

CRLINE 43 23 16

SF3CR 27 24 42 43 0

SFCOPY 27 27 1 5

VL2SF 6 28 27 1

c* Mesh volume for Inconel base

M_VL 6 6 1 8 16 16 1 80 16 1

c* Create Steel base

c* Create surfaces and volumes for the Steel base

CSANGL 6 0 0 0 3.937 0 0 0

ACTSET CS 0

SFCOPY 18 18 1 6

SFCOPY 19 19 1 6

VL2SF 7 32 18 1

VL2SF 8 33 19 1

c* Mesh volumes for Steel base

ACTSET EG 1

ACTSET MP 1

M_VL 7 7 1 8 16 4 1 80 16 1

M_VL 8 8 1 8 1 16 1 1 80 1

c* Create surface and volume for Steel disc

SFCOPY 28 28 1 6

VL2SF 9 41 28 1

c* Mesh volume for Steel disc

M_VL 9 9 1 8 16 16 1 80 16 1

c* Create rim for Steel base

CSANGL 7 0 0 0 6 0 0 0

ACTSET CS 0

SFCOPY 32 32 1 7

VL2SF 10 45 32 1

c* Mesh volume for Steel rim

M_VL 10 10 1 8 16 4 1 80 16 1

HIDDEN 1

VIEW -1 1 -1 0

SCALE 0

c* Merge nodes and compress elements

NMERGE,1,7000,1,0.0001,0,1,0,

NCOMPRESS,1,7000,1,

ECOMPRESS,1,5000,1,

c* Element group for gaps (4 nodes per surface)

EGROUP, 4, GAP, 1, 0, 0, 2, 4, , ,

RCONST 4 4 1 1 0

ACTSET EG 4

ACTSET RC 4

NL_GS 1 2576 2552 2479 2484

NL_GS 2 2552 2528 2474 2479

NL_GS 3 2528 2522 2381 2474

NL_GS 4 2577 2553 2552 2576

NL_GS 5 2553 2529 2528 2552

NL_GS 6 2529 2523 2522 2528

NL_GS 7 2578 2554 2553 2577

NL_GS 8 2554 2530 2529 2553

NL_GS 9 2530 2524 2523 2529

EL, ,PT,0,1,2382,

EL, ,PT,0,1,2383,

EL, ,PT,0,1,2384,

EL, ,PT,0,1,2385,

EL, ,PT,0,1,2386,

EL, ,PT,0,1,2296,

EL, ,PT,0,1,2297,

EL, ,PT,0,1,2298,

EL, ,PT,0,1,2299,

EL, ,PT,0,1,2300,

EL, ,PT,0,1,2301,

EL, ,PT,0,1,2211,

EL, ,PT,0,1,2212,

EL, ,PT,0,1,2213,

EL, ,PT,0,1,2214,

EL, ,PT,0,1,2215,

EL, ,PT,0,1,2126,

EL, ,PT,0,1,2127,

EL, ,PT,0,1,2128,

EL, ,PT,0,1,2129,

EL, ,PT,0,1,2130,

EL, ,PT,0,1,2041,

EL, ,PT,0,1,2042,

c* Plot gap surfaces

NL_GSPLOT;

c* Boudary conditions

c* Sphere &

c* Steel cylinder

DSF 6 UX 0 6 1

DSF 23 UX 0 23 1

DSF 33 UX 0 33 1

DSF 37 UX 0 37 1

DSF 39 UX 0 39 1

DSF 41 UX 0 44 1

DSF 44 UX 0 44 1

DSF 45 UX 0 45 1

DSF 49 UX 0 49 1

c* Inconel cylinder

DSF 16 UX 0 16 1

DSF 15 UX 0 15 1

DSF 25 UX 0 25 1

DSF 31 UX 0 31 1

c* Element group for the 2D trusses

EGROUP 5 TRUSS2D 0 0 0 0 0 0 0 0

RCONST 5 5 1 1 1

MPROP 5 EX 10E0

ACTSET EG 5

ACTSET RC 5

ACTSET MP 5

c* Create points and curves for truss elements to stabilize the sphere

PT 36 -2 0 0

PT 37 -2 0 2

PT 38 -2 2 0

CRLINE 74 36 1

CRLINE 75 37 12

CRLINE 76 38 11

c* Mesh curves for the trusses

M_CR 74 76 1 2 1 1

NMERGE,1,7000 ,1,0.0001,0,1,0,

NCOMPRESS,1,7000 ,1,

ECOMPRESS,1,5000 ,1,

c* Boundary conditions for the trusses

DPT 36 UX 0 38 1

c* Restrict motion of every node in Y and Z directions

DND,1,UY,0,6000 ,1,UZ,

c* Define Force Time curve

TIMES 0 1 0.1

CURDEF TIME 1 1 0 0 1 1

ACTSET TC 1

c* Force on Sphere Total = 21000 lbf (21 nodes)

FSF 8 FX 1000 8 1

c* Print displacements

PRINT_OPS 1 0 0 0 0 0 0 1 0

c* Define group of nodes for which Displacements will be written

PRINT_NDSET 10 1956 1961 2041 2046 2126 2131 2211 2216 2296 2301 2381

2386 2474 2484 2522 2530 2552 2554 2576 2578

c* Define group of elements for which Stresses will be written

PRINT_ELSET 8 1473 1477 1537 1541 1601 1605 1665 1669 1729 1733 1811

1813 1835 1837 1859 1861

c* Non linear solution

NL_SOLN 1 0

NL_PLOT 1,10,1

c* Run Nonlinear analysis

R_NONLINEAR

APPENDIX V

FORTRAN PROGRAM TO CALCULATE STRESS* VOLUME

C FORTRAN Program to calculate the product, Stress * Volume

C Data is directly read from the COSMOS/M output file

C Declare Variables

DOUBLE PRECISION X(600),Y(600),Z(600),UX(600),UY(600),UZ(600)

DOUBLE PRECISION P1(600),Q1(600),R1(600),P2(600),Q2(600),R2(600)

DOUBLE PRECISION P3(600),Q3(600),R3(600),P4(600),Q4(600),R4(600)

DOUBLE PRECISION XX(600),YY(600),ZZ(600),PP1(600),QQ1(600)

DOUBLE PRECISION RR1(600),PP2(600),QQ2(600),RR2(600),PP3(600)

DOUBLE PRECISION QQ3(600),RR3(600),PP4(600),QQ4(600),RR4(600)

DOUBLE PRECISION V(6000),VOL(6000),ELEVOL(6000),ALPHA(600)

DOUBLE PRECISION VOLSTP(6000),SIGX(6000),SXVOL(6000),SV(6000)

DOUBLE PRECISION STSXVOL(6000),SUM(6000),CE(300),NM

DOUBLE PRECISION P(600),Q(600),R(600),ELSIGVOL(6000),INCF

DOUBLE PRECISION ST1(600),ST2(600),ST3(600),ST4(600),AVGST(600)

DOUBLE PRECISION FORCE,FR(600),KS,PW,U1(600),U2(600),U3(600)

DOUBLE PRECISION DU1(2000),DU2(2000),DU3(2000)

```
INTEGER N(600),ELMT(600),N1(600),N2(600),N3(600),N4(600),A
```

```
INTEGER L,E,F
```

```
INTEGER C1,C2,C3,C4,C5,C6,I,K,J,H
```

```
CHARACTER CH1(600),CH2(600),CH3(600),CH4(600)
```

C Open data files and output files

```
OPEN (UNIT=1,FILE='dataf8.dat',STATUS='OLD')
```

```
OPEN (UNIT=2,FILE='d.dat',STATUS='OLD')
```

```
OPEN (UNIT=42,FILE='s1.dat',STATUS='OLD')
```

```
OPEN (UNIT=43,FILE='s2.dat',STATUS='OLD')
```

```
OPEN (UNIT=44,FILE='s3.dat',STATUS='OLD')
```

```
OPEN (UNIT=45,FILE='e.dat',STATUS='OLD')
```

```
OPEN (UNIT=82,FILE='nsgv8.out',STATUS='OLD')
```

C Read coordinates of nodes

```
DO 5 I=1,36
```

```
    READ(1,2)N(I),C1,C2,C3,C4,C5,C6,X(I),Y(I),Z(I)
```

```
2    FORMAT(I6,I7,I5,I5,I5,I5,I5,E12.5,E13.5,E18.5)
```

```
    P(I)=X(I)
```

```
    Q(I)=Y(I)
```

```
    R(I)=Z(I)
```

```
5    CONTINUE
```

```
    P(37)=X(31)
```

```
    Q(37)=Y(31)
```

R(37)=Z(31)

DO 6 I=38,52,1

READ(1,2)N(I),C1,C2,C3,C4,C5,C6,X(I),Y(I),Z(I)

U1(I)=X(I)

U2(I)=Y(I)

U3(I)=Z(I)

6 CONTINUE

P(38)=U1(38)

Q(38)=U2(38)

R(38)=U3(38)

P(39)=U1(39)

Q(39)=U2(39)

R(39)=U3(39)

P(40)=U1(40)

Q(40)=U2(40)

R(40)=U3(40)

P(41)=U1(41)

Q(41)=U2(41)

R(41)=U3(41)

P(42)=U1(44)

Q(42)=U2(44)

R(42)=U3(44)

P(43)=U1(47)

Q(43)=U2(47)

R(43)=U3(47)

P(44)=U1(50)

Q(44)=U2(50)

R(44)=U3(50)

P(45)=U1(42)

Q(45)=U2(42)

R(45)=U3(42)

P(46)=U1(45)

Q(46)=U2(45)

R(46)=U3(45)

P(47)=U1(48)

Q(47)=U2(48)

R(47)=U3(48)

P(48)=U1(51)

Q(48)=U2(51)

R(48)=U3(51)

P(49)=U1(43)

Q(49)=U2(43)

R(49)=U3(43)

P(50)=U1(46)

```
Q(50)=U2(46)
R(50)=U3(46)
P(51)=U1(49)
Q(51)=U2(49)
R(51)=U3(49)
P(52)=U1(52)
Q(52)=U2(52)
R(52)=U3(52)
DO 7 I=37,52,1
    X(I)=P(I)
    Y(I)=Q(I)
    Z(I)=R(I)
7 CONTINUE
DO 30 M=1,20
    DO 10 I=1,36
        READ(1,8)N(I),UX(I),UY(I),UZ(I)
8    FORMAT(I6,E14.4,E12.5,E12.5)
        XX(I)=P(I)+UX(I)
        YY(I)=Q(I)+UY(I)
        ZZ(I)=R(I)+UZ(I)
10 CONTINUE
WRITE(43,12)UX(31)
```

12 FORMAT(F15.9)

A=7

J=1

K=1

DO 15 I=1,25

P1(J)=X(A)

PP1(J)=XX(A)

Q1(J)=Y(A)

QQ1(J)=YY(A)

R1(J)=Z(A)

RR1(J)=ZZ(A)

P2(J)=X(K)

PP2(J)=XX(K)

Q2(J)=Y(K)

QQ2(J)=YY(K)

R2(J)=Z(K)

RR2(J)=ZZ(K)

P3(J)=X(K+1)

PP3(J)=XX(K+1)

Q3(J)=Y(K+1)

QQ3(J)=YY(K+1)

R3(J)=Z(K+1)

```
RR3(J)=ZZ(K+1)
```

```
P4(J)=X(A+1)
```

```
PP4(J)=XX(A+1)
```

```
Q4(J)=Y(A+1)
```

```
QQ4(J)=YY(A+1)
```

```
R4(J)=Z(A+1)
```

```
RR4(J)=ZZ(A+1)
```

C Write coordinates of elements into data file

```
WRITE(2,14)P1(J),Q1(J),R1(J)
```

```
WRITE(2,14)P2(J),Q2(J),R2(J)
```

```
WRITE(2,14)P3(J),Q3(J),R3(J)
```

```
WRITE(2,14)P4(J),Q4(J),R4(J)
```

```
WRITE(2,14)PP1(J),QQ1(J),RR1(J)
```

```
WRITE(2,14)PP2(J),QQ2(J),RR2(J)
```

```
WRITE(2,14)PP3(J),QQ3(J),RR3(J)
```

```
WRITE(2,14)PP4(J),QQ4(J),RR4(J)
```

```
14 FORMAT(F25.10,F25.10,F25.10)
```

```
K=K+1
```

```
A=A+1
```

```
J=J+1
```

```
IF (J.EQ.6) THEN
```

```
    J=1
```



```
                A=A+1
                K=K+1
            END IF
15  CONTINUE
    DO 20 I=1,36
        X(I)=XX(I)
        Y(I)=YY(I)
        Z(I)=ZZ(I)
20  CONTINUE
        N(37) = N(31)
        DU1(37) = UX(31)
        DU2(37) = UY(31)
        DU3(37) = UZ(31)
    DO 21 H=38,52,1
        READ(1,8)N(H),DU1(H),DU2(H),DU3(H)
21  CONTINUE
        UX(37)=DU1(37)
        UY(37)=DU2(37)
        UZ(37)=DU3(37)
        UX(38)=DU1(38)
        UY(38)=DU2(38)
        UZ(38)=DU3(38)
```

UX(39)=DU1(39)

UY(39)=DU2(39)

UZ(39)=DU3(39)

UX(40)=DU1(40)

UY(40)=DU2(40)

UZ(40)=DU3(40)

UX(41)=DU1(41)

UY(41)=DU2(41)

UZ(41)=DU3(41)

UX(42)=DU1(44)

UY(42)=DU2(44)

UZ(42)=DU3(44)

UX(43)=DU1(47)

UY(43)=DU2(47)

UZ(43)=DU3(47)

UX(44)=DU1(50)

UY(44)=DU2(50)

UZ(44)=DU3(50)

UX(45)=DU1(42)

UY(45)=DU2(42)

UZ(45)=DU3(42)

UX(46)=DU1(45)

UY(46)=DU2(45)

UZ(46)=DU3(45)

UX(47)=DU1(48)

UY(47)=DU2(48)

UZ(47)=DU3(48)

UX(48)=DU1(51)

UY(48)=DU2(51)

UZ(48)=DU3(51)

UX(49)=DU1(43)

UY(49)=DU2(43)

UZ(49)=DU3(43)

UX(50)=DU1(46)

UY(50)=DU2(46)

UZ(50)=DU3(46)

UX(51)=DU1(49)

UY(51)=DU2(49)

UZ(51)=DU3(49)

UX(52)=DU1(52)

UY(52)=DU2(52)

UZ(52)=DU3(52)

DO 22 I=37,52

XX(I)=P(I)+UX(I)

$$YY(I)=Q(I)+UY(I)$$
$$ZZ(I)=R(I)+UZ(I)$$

22 CONTINUE

$$A=41$$
$$J=1$$
$$K=37$$

DO 23 I=1,9

$$P1(J)=X(A)$$
$$PP1(J)=XX(A)$$
$$Q1(J)=Y(A)$$
$$QQ1(J)=YY(A)$$
$$R1(J)=Z(A)$$
$$RR1(J)=ZZ(A)$$
$$P2(J)=X(K)$$
$$PP2(J)=XX(K)$$
$$Q2(J)=Y(K)$$
$$QQ2(J)=YY(K)$$
$$R2(J)=Z(K)$$
$$RR2(J)=ZZ(K)$$
$$P3(J)=X(K+1)$$
$$PP3(J)=XX(K+1)$$
$$Q3(J)=Y(K+1)$$

```
QQ3(J)=YY(K+1)
R3(J)=Z(K+1)
RR3(J)=ZZ(K+1)
P4(J)=X(A+1)
PP4(J)=XX(A+1)
Q4(J)=Y(A+1)
QQ4(J)=YY(A+1)
R4(J)=Z(A+1)
RR4(J)=ZZ(A+1)
WRITE(2,14)P1(J),Q1(J),R1(J)
WRITE(2,14)P2(J),Q2(J),R2(J)
WRITE(2,14)P3(J),Q3(J),R3(J)
WRITE(2,14)P4(J),Q4(J),R4(J)
WRITE(2,14)PP1(J),QQ1(J),RR1(J)
WRITE(2,14)PP2(J),QQ2(J),RR2(J)
WRITE(2,14)PP3(J),QQ3(J),RR3(J)
WRITE(2,14)PP4(J),QQ4(J),RR4(J)
K=K+1
A=A+1
J=J+1
IF (J.EQ.4) THEN
    J=1
```

A=A+4

K=K+4

END IF

23 CONTINUE

DO 24 I=37,52

X(I)=XX(I)

Y(I)=YY(I)

Z(I)=ZZ(I)

24 CONTINUE

C Write average stress into data file

DO 28 I=1,34

READ(1,*)ELMT(I)

READ(1,25)N1(I),CH1(I),ST1(I)

25 FORMAT(I10,A9,E11.4)

READ(1,25)N2(I),CH2(I),ST2(I)

READ(1,*)

READ(1,*)

READ(1,25)N3(I),CH3(I),ST3(I)

READ(1,25)N4(I),CH4(I),ST4(I)

READ(1,*)

READ(1,*)

AVGST(I)=0.25*(ST1(I)+ST2(I)+ST3(I)+ST4(I))

```
        WRITE(42,26)ELMT(I),AVGST(I)
26   FORMAT(I8,1X,F15.3)
28   CONTINUE
30   CONTINUE

        CLOSE (2)

        CLOSE (42)

        CLOSE (43)

        OPEN(UNIT=2,FILE='d.dat',STATUS='OLD')
        OPEN(UNIT=42,FILE='s1.dat',STATUS='OLD')
        OPEN(UNIT=43,FILE='s2.dat',STATUS='OLD')

C   Declare Force

        FORCE=2100.0

C   Number of Increments

        NM=20.0

C   Force increment

        INCF=(FORCE)/(NM)

C   Initialize counters

        J=1

        F=1

C   Define Stiffness constant and power index

        KS=847751.0

        PW=1.0
```

```

35 FORMAT(5X,'K = ',F10.2,2X,'n = ',F8.5,2X,'Force = ',F10.2,
$2X,'No of steps = ',F5.1,/)
WRITE(44,35)KS,PW,FORCE,NM

```

C Force value at zero step

```

40 FORMAT(7X,'Alpha',10X,'Force',11X,'K*Alpha**n',9X,
$'Sig*Vol',6X,'Fm*Alpha/(n+1)',/)
WRITE(44,40)
FR(F-1)=0.0
CE(F-1)=0.0
ALPHA(F-1)=0.0
SV(F-1)=0.0
SUM(F-1)=0.0
STXVOL(F-1)=0.0
WRITE(44,145)ALPHA(F-1),CE(F-1),FR(F-1),
$SUM(F-1),SV(F-1),STXVOL(F-1)
DO 45 I=1,20
    CE(I)=CE(I-1)+INCF
45 CONTINUE

```

C Initialize variables

```

F=1
L=0
VOL(J)=0.0

```



```
ELEVOL(J)=0.0
```

```
ELSIGVOL(J)=0.0
```

```
SXVOL(J)=0.0
```

```
VOLSTP(F)=0.0
```

```
STSXVOL(F)=0.0
```

```
80 FORMAT ('Tetrahedron number = ',I3,4X,'Volume = ',F15.8)
```

```
85 FORMAT ('Sigma X = ',F15.2,4X,'Sigma_X * Volume = ',
$F15.6,/)

```

C Read the X, Y, Z coordinates of each node, from the

C data file in order

```
DO 150 E=1,20
```

```
I = 1
```

```
V(I) = 0.0
```

```
DO 120 L=(L+ 1),(34 + L)
```

C Open Elements file and read the data

```
READ(42,*)ELMT(L),SIGX(L)
```

C Read 8 nodes at a time from the data file

```
DO 90 K=1,8
```

```
READ(2,14)X(K),Y(K),Z(K)
```

```
90 CONTINUE
```

C Calculate the volume of the 1st Tetrahedron

```
V(I) = TETRA(X(1),X(4),X(5),X(6),Y(1),Y(4),Y(5),Y(6),
```

\$Z(1),Z(4),Z(5),Z(6))

VOL(J) = VOL(J) + V(I)

ELEVOL(J) = ELEVOL(J) + V(I)

WRITE (82, 80) I, V(I)

C Calculate the volume of the 2nd Tetrahedron

I = I + 1

V(I) = 0.0

V(I) = TETRA(X(2),X(6),X(4),X(3),Y(2),Y(6),Y(4),Y(3),

\$Z(2),Z(6),Z(4),Z(3))

VOL(J) = VOL(J) + V(I)

ELEVOL(J) = ELEVOL(J) + V(I)

WRITE (82, 80) I, V(I)

C Calculate the volume of the 3rd Tetrahedron

I = I + 1

V(I) = 0.0

V(I) = TETRA(X(2),X(4),X(6),X(1),Y(2),Y(4),Y(6),Y(1),

\$Z(2),Z(4),Z(6),Z(1))

VOL(J) = VOL(J) + V(I)

ELEVOL(J) = ELEVOL(J) + V(I)

WRITE (82, 80) I, V(I)

C Calculate the volume for the 4th Tetrahedron

I = I + 1

$$V(I) = 0.0$$

$$V(I) = \text{TETRA}(X(4), X(5), X(8), X(6), Y(4), Y(5), Y(8), Y(6), \\ \$Z(4), Z(5), Z(8), Z(6))$$

$$\text{VOL}(J) = \text{VOL}(J) + V(I)$$

$$\text{ELEVOL}(J) = \text{ELEVOL}(J) + V(I)$$

$$\text{WRITE (82, 80) I, V(I)}$$

C Calculate the volume of the 5th Tetrahedron

$$I = I + 1$$

$$V(I) = 0.0$$

$$V(I) = \text{TETRA}(X(4), X(7), X(6), X(8), Y(4), Y(7), Y(6), Y(8), \\ \$Z(4), Z(7), Z(6), Z(8))$$

$$\text{VOL}(J) = \text{VOL}(J) + V(I)$$

$$\text{ELEVOL}(J) = \text{ELEVOL}(J) + V(I)$$

$$\text{WRITE (82, 80) I, V(I)}$$

C Calculate the volume of the 6th Tetrahedron

$$I = I + 1$$

$$V(I) = 0.0$$

$$V(I) = \text{TETRA}(X(4), X(6), X(7), X(3), Y(4), Y(6), Y(7), Y(3), \\ \$Z(4), Z(6), Z(7), Z(3))$$

$$\text{VOL}(J) = \text{VOL}(J) + V(I)$$

$$\text{ELEVOL}(J) = \text{ELEVOL}(J) + V(I)$$

$$\text{ELSIGVOL}(J) = \text{SIGX}(L) * \text{ELEVOL}(J)$$

SXVOL(J) = SXVOL(J) + ELSIGVOL(J)

VOLSTP(F) = VOLSTP(F) + ELEVOL(J)

STSVOL(F) = STSVOL(F) + ELSIGVOL(J)

WRITE (82, 80) I, V(I)

V(I) = 0.0

100 FORMAT (/,'Element number = ',I5,4X,'Volume = ',F15.10,/))

C Calculate the volume of the next Element

I = 1

J = J + 1

VOL(J) = VOL(J-1)

SXVOL(J) = SXVOL(J-1)

C Write the volume of the element in the output file

WRITE (82, 100) ELMT(L), ELEVOL(J-1)

WRITE (82, 85) SIGX(L), ELSIGVOL(J-1)

C Reset the variables

ELEVOL(J) = 0.0

ELSIGVOL(J) = 0.0

120 CONTINUE

125 FORMAT (/,'*****')

\$(*****')

130 FORMAT (/,'*',4X,'step number = ',I3,7X,'Volume of deformation = ',

\$F13.10,2X,'in^3',5X,'*',/)

```
135 FORMAT ('*****',3X,'STEP TOTAL Sigma_X * Volume = ',
           '$F10.3,3X,'*****',/)
```

```
136 FORMAT ('*
           $          *)
           WRITE (82, 125)
           WRITE (82, 136)
           WRITE (82, 130) F, VOLSTP(F)
           WRITE (82, 136)
           WRITE (82, 135) STSXVOL(F)
           SUM(F) = SUM(F-1)+STSXVOL(F)
```

C Increment the Step number

F = F + 1

```
140 FORMAT ('***** Sum Total = ',
           '$F10.3,3X,'*****',/)
```

```
           WRITE (82, 140) SUM(F-1)
           READ (43, *) ALPHA(F-1)
           FR(F-1) = KS*((ALPHA(F-1))** PW)
           SV(F-1) = ( FR(F-1) * ALPHA(F-1))/(1.0+PW)
```

```
145 FORMAT (F15.9,2X,F15.3,2X,F15.3,2X,F15.9,2X,F15.9,2X,F15.9)
           WRITE (44, 145) ALPHA(F-1),CE(F-1),FR(F-1),
           $(-1.0*SUM(F-1)),SV(F-1),(-1.0*STSXVOL(F-1))
```

150 CONTINUE

C Write the Total volume of deformation into the output file

200 FORMAT (//,'Total volume of deformation = ',F15.12)

205 FORMAT (/,'Total Sigma_X * Volume = ',F12.2)

WRITE (82, 200) VOL(J-1)

210 CONTINUE

WRITE (82, 205) SXVOL(J-1)

C Close the initial coordinate file

CLOSE (1)

C Close the data file

CLOSE (2)

CLOSE (42)

CLOSE (43)

CLOSE (44)

C Close output file

CLOSE (82)

STOP

END

C Function to calculate the volume of a Tetrahedron

REAL FUNCTION TETRA (A1,A2,A3,A4,B1,B2,B3,B4,C1,C2,C3,C4)

DOUBLE PRECISION A1,A2,A3,A4,B1,B2,B3,B4,C1,C2,C3,C4

TETRA = ABS(((B2-B1)*(C3-C1)-(B3-B1)*(C2-C1))*(A4-A1)+((A3-A1)*

$$(C2-C1)-(A2-A1)*(C3-C1))*(B4-B1)+((A2-A1)*(B3-B1)-(A3-A1)*$

$$(B2-B1))*(C4-C1))/6.0$

RETURN

END

APPENDIX VI

TABLES OF DATA

Table 3.3.2

Force (lbf)	Displacement (in)
0	0
82	0.00002133
164	0.00004266
246	0.00006399
328	0.00008533
410	0.00010660
492	0.00012800
574	0.00014930
656	0.00017060
738	0.00019190
820	0.00021330

Table 3.3.4

Gap Height (in)	Displacement (in)	Stress (lbf/in ²)
0	0	0
0.015821	0.00056413	1.1656×10^5
0.033007	0.0012485	1.3734×10^5
0.051671	0.0022094	1.4132×10^5
0.051671	0.0031218	1.6552×10^5
0.071929	0.0040605	1.6151×10^5
0.071929	0.0055726	1.8652×10^5
0.093906	0.0064249	1.7528×10^5
0.093906	0.0081153	1.9843×10^5
0.117733	0.0093609	1.8908×10^5
0.117733	0.0108800	1.9681×10^5

Table 4.3.1

Force (lbf)	Displacement (in)
0	0
136.5	0.000161
273	0.000322
409.5	0.000483
546	0.000644
682.5	0.000805

Table 4.3.4

Displacement (in)	Stress*Volume (lbf.in)
0	0
0.000495	0.265
0.001033	0.833
0.001950	2.242
0.003136	4.698
0.004464	8.142
0.005860	12.485
0.007564	18.596
0.009683	27.205
0.012066	38.113
0.014690	51.441

APPENDIX VII

MATHCAD CALCULATIONS FOR SPHERE AND CYLINDER

FEM determination of $\alpha.p$ using a given Impact Velocity

MathCad Solution

Density of Steel Density of Inconel

$$\rho_{st} := 0.2799 \text{ lbm/in}^3 \quad \rho_{inc} := 0.2731 \text{ lbm/in}^3$$

Volume of sphere

$$V_{sph} := \frac{4}{3} \cdot \pi \cdot \frac{2^3}{8}$$

$$V_{sph} = 4.18879 \text{ in}^3$$

Volume of Steel cylinder

$$V_{st} := \pi \cdot (29.606^2 - 25.669^2) \cdot \frac{110.236}{4} + \pi \cdot 25.669^2 \cdot \frac{3.937}{4}$$

$$V_{st} = 2.08785410^4 \text{ in}^3$$

Volume of Inconel cylinder

$$V_{inc} := \pi \cdot (25.669^2 - 25.299^2) \cdot \frac{99.925}{4} + \pi \cdot 25.669^2 \cdot \frac{0.374}{4}$$

$$V_{inc} = 1.68943210^3 \text{ in}^3$$

Equivalent Mass of system

$$m1 := V_{sph} \cdot \rho_{st}$$

$$m2 := V_{st} \cdot \rho_{st} + V_{inc} \cdot \rho_{inc}$$

$$M := \frac{m1 \cdot m2}{m1 + m2}$$

$$M = 1.172224 \quad \text{lbm}$$

$$n := 1 \quad K := 847751 \quad \text{lbf/in}$$

Minimum velocity to produce plastic deformation

$$F_p := 887.25 \quad \text{lbf}$$

$$V_p := \sqrt{\frac{F_p}{K} \cdot \frac{n+1}{n} \cdot \frac{1}{2} \cdot \frac{1}{n+1} \cdot \frac{1}{M}}$$

$$V_p = 0.890034 \quad \text{in/sec}$$

$$V_{mph} := V_p \cdot \frac{3600}{5280 \cdot 12}$$

$$V_{mph} = 0.05057 \quad \text{mph}$$

Input initial velocity

$$i := 1, 2, \dots, 100$$

$$v_{mph_i} := i \cdot 0.005 \quad \text{Valid speed range 0.08 mph to 0.369 mph}$$

$$v_i := \frac{v_{mph_i}}{3600} \cdot 5280 \cdot 12$$

$$\alpha_{mf_i} := \left[\frac{1}{2} \cdot M \cdot \left(v_i \right)^2 \cdot \frac{n+1}{K} \right]^{\frac{1}{n+1}}$$

Force of impact

$$Fmf_i := K \cdot (\alpha mf_i)^n$$

Evaluate αp

$$\alpha pr := 0.1 \quad \text{Guess value} \quad j := 10..80 \quad z_j := j \cdot 0.001$$

$$\alpha pf_j := \text{root} \left[\left[4.1889410^8 \cdot (\alpha pr)^4 - 1.0358910^7 \cdot (\alpha pr)^3 + 205948(\alpha pr)^2 + 2087.91\alpha pr \right] - Fmf_j \cdot \frac{\alpha pr}{n+1}, \alpha pr \right]$$

Coefficient of Restitution

$$ef_j := \sqrt{1 - \frac{\alpha pf_j}{\alpha mf_j}}$$

Time of duration in the compression stage

$$\tau_{1j} := \frac{\alpha mf_j}{v_j} \int_0^1 \frac{1}{\sqrt{1 - u^{n+1}}} du$$

Time of duration in the restitution phase

$$\tau_{2j} := \frac{\alpha mf_j - \alpha pf_j}{v_j \cdot ef_j} \int_0^1 \frac{1}{\sqrt{1 - u^{n+1}}} du$$

BIBLIOGRAPHY

1. Barnhart, K. E., Goldsmith, W., "Stresses in Beams during Transverse Impact," ASME Journal of Applied Mechanics, September 1957, Vol. 24, pp. 440-446.
2. Brach, R. M., "Mechanical Impact Dynamics: Rigid Body Collisions," John Wiley & Sons, New York, 1991.
3. Cook, R. D., Malkus, D. S. and Plesha, M. E., "Concepts and applications of finite element analysis," John Wiley & Sons, New York, 1989, Third edition.
4. Crook, A. W., "A Study of Some Impacts Between Metal Bodies by a Piezo-Electric Method," Royal Society, London, 1952, Vol. A, No. 212, pp. 377-390.
5. Deresiewicz, H., "A Note on Hertz's Theory of Impact," Acta Mechanica, 1968, No. 6, pp. 110-112.
6. Easley, J.G., "Mechanics of Elastic Structures - classical and finite element methods," Prentice Hall, New Jersey, 1989.
7. Goldsmith, W., "Impact, the Theory and Physical Behaviour of Colliding Solids," Edward Arnold Ltd., 1960.
8. Johnson, K. L., "Contact Mechanics," Cambridge University Press, 1985.
9. Khulief, Y. A., Shabana, A. A., "Impact Response of Multi-Body Systems with Consistent and Lumped Masses," Journal of Sound and Vibration (1986), 104(2), pp. 187-207.
10. Khulief, Y. A., Shabana, A. A., "A Continuous Force Model for the Impact Analysis of Flexible Multibody Systems," Mech. Mach. Theory, Vol. 22, No.3, pp. 213-224, 1987.
11. Lankarani, H. M., Nikravesh, P. E., "Hertz Contact Force Model with Permanent Indentation in Impact Analysis of Solids," Advances in Design Automation - Volume 2, DE-Vol. 44-2, ASME 1992, pp. 391-395.

12. Lankarani, H. M., Nikraves, P. E., "*Canonical Impulse-Momentum Equations for Impact Analysis of Multibody Systems*," Transactions of the ASME, Journal of Mechanical Design, Vol. 114, March 1992, pp. 180-186.
13. Meirovitch, L., "*Methods of Analytical Dynamics*," McGraw-Hill Book Company, New York, 1970.
14. Structural Research and Analysis Corporation, "*COSMOS/M*," Version 1.7, 1994, Geostar user guide, user guide vol.1 and vol.2, California.
15. Young, W. C., "*Roark's Formulas for Stress and Strain*," McGraw-Hill Book Company, New York, 1989, sixth edition.